2021-04-02

The ssDNA Theory of BRCAness and Genotoxic Agents

Nicholas J. Panzarino
University of Massachusetts Medical School

THE ssDNA THEORY OF *BRCAness* AND GENOTOXIC AGENTS

A Dissertation Presented

By

NICHOLAS JOHN PANZARINO

Submitted to the Faculty of the

University of Massachusetts Graduate School of Biomedical Sciences, Worcester

in partial fulfillment of the requirements for the degree of

DOCTOR OF PHILOSOPHY

APRIL 2, 2021

CANCER BIOLOGY

THE ssDNA THEORY OF *BRCAness* AND GENOTOXIC AGENTS

A Dissertation Presented

By

NICHOLAS JOHN PANZARINO

This work was undertaken in the Graduate School of Biomedical Sciences

Cancer Biology Graduate Program

Under the mentorship of

_____

Sharon Cantor, Ph.D., Thesis Advisor

_____

Paul Kaufman, Ph.D., Member of Committee

_____

Kendall Knight, Ph.D., Member of Committee

_____

Michael Lee, Ph.D., Member of Committee

_____

Alessandro Vindigni, Ph.D., External Member of Committee

_____

Craig Ceol, Ph.D., Chair of Committee

_____

Mary Ellen Lane, Ph.D.,

Dean of the Graduate School of Biomedical Sciences

April 2, 2021

DEDICATION

To Olivia

ACKNOWLEDGEMENTS

I am grateful to my adviser, Sharon Cantor, for the opportunity to pursue a Ph.D. in her group and for creating an environment where meaningful research could occur. I believe what we accomplished holds great promise to help heal the sick, and I very much hope to see these opportunities come to fruition. Similarly, I am grateful to my committee, including Craig Ceol, Paul Kaufman, Kendall Knight, Michael Lee, and Craig Peterson, for their expertise and contributions that very much helped to shape our work into the promising theory it would become. I am also indebted to the graduate program, specifically Kendall Knight, Anthony Carruthers, and Art Mercurio, for the opportunity to begin a Ph.D. at the University of Massachusetts Medical School. I also need to thank our outstanding collaborators, including members of the Cantor Lab, as well as John Krais, Neil Johnson, Bin Deng, Jianhong Ou, Julie Zhu, and Alessandro Vindigni for their important contributions to the paper.

Finally, my work would not have been possible without the foundation I received from Sallie Schneider, Todd Emrick, and Rick Arenas at the University of Massachusetts Amherst, as well as the support I received from my family.

And, of course, for P.G. – thank you for the shot.

ABSTRACT

Cancers that are deficient in BRCA1 or BRCA2 are thought to be hypersensitive to genotoxic agents because they cannot prevent or repair DNA double strand breaks, but observations in patients suggest this dogma may no longer agree with experiment. Here, we propose that single stranded DNA underlies the hypersensitivity of BRCA deficient cancers, and that defects in double strand break repair and prevention do not. Specifically, in BRCA deficient cells, ssDNA gaps developed because replication was not effectively restrained in response to stress. In addition, we observed gaps could be suppressed by either restored fork restraint or by gap filling, both of which conferred therapy resistance in tissue culture and BRCA patient tumors. In contrast, restored double strand break repair and prevention did not confer therapy resistance when gaps were present. Critically, double strand breaks were not detected after therapy when apoptosis was inhibited, supporting a framework in which double strand breaks are not directly induced by genotoxic agents, but instead are created by cell death nucleases and are not fundamental to genotoxic agents. Together, these data indicate that ssDNA replication gaps underlie the BRCA cancer phenotype, "*BRCAness*," and we propose are fundamental to the mechanism-of-action of genotoxic chemotherapy.

TABLE OF CONTENTS

LIST OF TABLES

LIST OF FIGURES

LIST OF COPYRIGHTED MATERIALS PRODUCED BY THE AUTHOR

1. Panzarino, N. J. *et al.* Replication Gaps Underlie BRCA Deficiency and Therapy Response. *Cancer Res* **81**, 1388–1397 (2021).
2. Chaudhuri, A. R. *et al.* Replication fork stability confers chemoresistance in BRCA-deficient cells. *Nature* **535**, 382–7 (2016).

LIST OF THIRD PARTY COPYRIGHTED MATERIAL

CHAPTER I: INTRODUCTION

The ssDNA Theory of BRCAness and Genotoxic Agents

Summary: *This article introduces a new theory for the widespread female cancer phenotype known as BRCAness, a vulnerability that results in exquisite hypersensitivity to agents that damage DNA. We review the history of BRCAness and highlight how the new ssDNA theory accurately predicts therapy success while requiring less complexity than the established dogma. We also outline results that support the most surprising and provocative prediction of the theory: that the previous dogma for BRCAness may have been incorrectly based on an artifact generated by the programmed cell death machinery. We conclude with the consequences of the new framework for personalized medicine of BRCAness, cancer, and serious DNA metabolism-based disease.*

Genotoxins are poisons that damage DNA and therefore are ideal drugs to treat cancers that display the vulnerability known as *BRCAness*, in which defects in DNA metabolism lead to hypersensitivity to DNA damaging agents. Unfortunately, even in this ideal case for personalized medicine, the majority of *BRCAness* cancers will ultimately acquire resistance to genotoxic agents and progress to terminal disease.

Moreover, efforts to resensitize such cancers, or even to predict when drug resistance will occur in patients, have required adding substantial complexity to the established dogma, raising the exciting possibility that our understanding of genotoxins and *BRCAness* is not simply incomplete, but instead is fundamentally flawed.

Now, as described in this dissertation, a new theory proposes that it is single stranded DNA created by disrupted DNA replication, and not double strand breaks in the DNA as proposed by the dogma, that underlies the mechanism of action of genotoxins and represents the core defect of *BRCAness* (*Figure 1*). We propose this new ssDNA theory has forced a reconsideration of the established framework and could transformatively improve the therapies available for desperately ill patients.

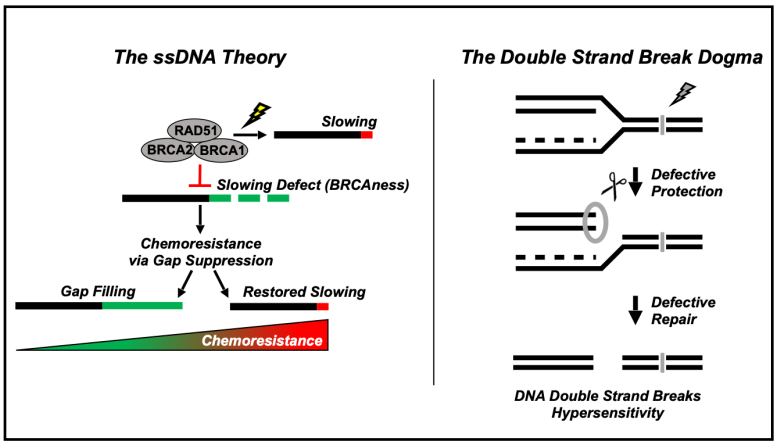

Figure 1.1: Comparison of The ssDNA Theory and The Double Strand Break Dogma. In the ssDNA model, the *BRCAness* proteins (gray) slow and arrest DNA replication after DNA damage (yellow lightning bolt). When these proteins are defective, replication fails to quickly arrest, leading to ssDNA that causes hypersensitivity (*BRCAness*). Chemoresistance is achieved when the ssDNA gaps are filled, or when slowing is restored. In the Double Strand Break Dogma, a DNA replication fork collides with damaged DNA (lightning bolt and gray bar). When the *BRCAness* proteins are defective, the DNA replication forks are cut (scissors, gray oval) and collapse into a double strand break (bottom) that cannot be effectively repaired, leading to hypersensitivity. Chemoresistance is achieved when the replication fork is protected from cutting to prevent double strand breaks from forming, or when repair of double strand breaks is restored.

The History of the BRCAness Dogma: Genetics

The *BRCAness* phenotype was first observed in cancer patients with mutated BRCA1 and BRCA2 as part of an effort to identify cancer susceptibility syndromes. These

patients were observed to have an inherited and increased risk of developing female cancers, which suggested that the BRCA genes suppressed tumors by metabolizing DNA to ensure genetic integrity[1–4]. Indeed, BRCA deficient cells were subsequently observed to display striking hypersensitivity to agents that, among various molecular targets, were found to damage DNA[5–8], many of which had been deployed as successful anti-cancer therapies in the clinic (Figure 1.2). Importantly, the hypersensitivity of BRCA cells to such agents not only confirmed that the BRCA proteins metabolized DNA as previously suspected[9,10], but also established, via complementary genetic evidence, that such therapies principally targeted DNA as their fundamental mechanism of action. Accordingly, these agents would ultimately become known as genotoxins - i.e. *genetic toxins* - and they remain essential chemotherapeutics for the majority of cancers even today[11].

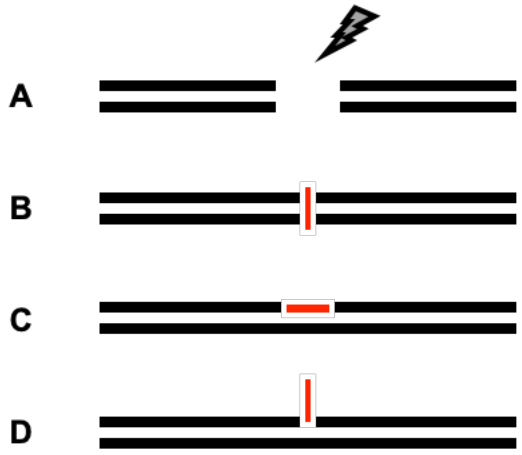

Figure 1.2: Genotoxic lesions. A, ionizing radiation breaks the DNA backbone directly, generating DNA double strand breaks as well as single strand breaks. B) Interstrand and C) intrastrand DNA crosslinks are created by agents with two functional groups available to bind DNA, such as cisplatin. D) DNA-protein adducts are created by agents such as camptothecin, which covalently traps the DNA replication protein topoisomerase I onto DNA, or PARPi, which traps the DNA repair protein called PARP. In addition, cisplatin also creates DNA-protein covalent linkages.

Out of the variety of DNA lesions created by genotoxins, the DNA double strand break dogma of *BRCAness* and hypersensitivity emerged from two key results: first, the BRCA

proteins were found to mediate a pathway called homologous recombination that repairs DNA double strand breaks, therefore suggesting that BRCA cells would be highly vulnerable to agents that generate such breaks[6,12,13]. Second, genotoxins were found to create extensive double strand breaks via pulsed field gel electrophoresis of treated cells[6,14–17], a result consistent with double strand breaks as the critical cellular lesions to drive the observed hypersensitivity in BRCA cancer.

Together, these results represented the core framework of the dogma: that DNA double strand breaks are the fundamental lesion of both *BRCAness* and genotoxic agents. However, although ionizing radiation had a straightforward mechanism of generating double strand breaks, the chemistry of genotoxins deployed against BRCAness cancers, for example cisplatin and camptothecin, only supported the creation of lesions such as adducts and crosslinks - not double strand breaks as a nuclease would create - and therefore required adopting a more complex framework[18–20]. Similarly, it was found that inhibiting the DNA repair protein called PARP conferred synthetic lethality in BRCA cells and was a targeted, specific therapy for BRCAness[21,22], but a mechanism for PARPi generating double strand breaks was unclear. Mechanistically, PARP was a protein involved in DNA repair that was responsible for signaling via ADP-ribosylation in the DNA damage response - how could inhibiting PARP, or creating adducts on DNA, create extensive double strand breaks to generate hypersensitivity in BRCA cancers?

The BRCAness Dogma Adds DNA Replication Forks

Ultimately, the key precursor to double strand breaks was proposed to be a replication fork that collides with a DNA lesion[5,21–23]; this model was supported by several important results. First, the replication fork presents a vulnerable region of DNA that could, in principle, collapse at a lesion and create a DNA double strand break[16,21,22] (*Figure 1, gray oval)*. Second, homologous recombination via the BRCA proteins is largely only active when cells are replicating, indicating that the BRCA vulnerability might manifest at a fork[16,21,22]. Finally, sensitivity to genotoxins was only observed when cells were actively replicating; indeed, genotoxins were found to be broadly less effective when cells were arrested, with toxicity reduced by three to ten fold depending on the specific agent used[16,21,22].

Importantly, strong experimental support for this framework was found in pulsed field gel electrophoresis experiments with camptothecin[16]. Indeed, camptothecin was observed to create double strand breaks at nascent DNA, which suggested the breaks were created at the replication fork. Moreover, the observed double strand breaks were eliminated upon co-treatment with aphidocholin, an antibiotic inhibitor of DNA polymerase; this role for replication further suggested that the camptothecin lesions had in fact collapsed a fork into a double strand break. Critically, this broken-fork principle was consistent with the chemistry of other genotoxins, all of which created replication disrupting lesions, including cisplatin and PARPi, and could explain their hypersensitivity in BRCA cells via double strand breaks. Indeed, a similar concept to camptothecin was developed for PARPi, which was proposed to create a vulnerable single stranded region at the replication fork that would cause forks to collapse into a double strand break[21].

Taken together, these results added the collapsed replication fork to the double strand break dogma of BRCAness as illustrated in *Figure 1*, and would ultimately lead to the important idea that forks could be degraded or stabilized to determine therapy success[21,22].

Replication Fork Degradation and Stabilization

The collapsed-fork model predicted several phenotypes that were experimentally confirmed and therefore largely solidified the dogma. First, the framework suggested that the forks of BRCA deficient cells would be more unstable and therefore prone to collapsing into double strand breaks at sites of DNA damage to exacerbate the hypersensitivity phenotype. This prediction was confirmed by Schlacher et al.[24,25], where they reported that BRCA forks were degraded by the nuclease MRE11 after being exposed to genotoxins, whereas BRCA proficient forks were protected. These results revealed that, not only were BRCA cells deficient for repairing DNA double strand breaks, but they also appeared more prone to generating them.

Secondly, the framework predicted that, if the replication fork could be protected, double strand breaks would be prevented from forming and resistance would be conferred, even in the absence of proficient double strand break repair via homologous recombination. This phenotype was confirmed by Chaudhuri et al.[26], where they observed a number of genes that, when depleted, stabilized BRCA replication forks in DNA fiber assays and eliminated MRE11 chromatin localization. Moreover, these genes

were observed to confer chemoresistance in BRCA cells when depleted but, as predicted by the framework, did not restore homologous recombination for double strand break repair[26,27].

These key observations represented the final aspects of the dogma and led to the complete and elegant double strand break framework shown in *Figure 1*. Other groups identified additional genes that protected forks and conferred chemoresistance in BRCA cells when depleted and found these genes accurately predicted BRCA cancer patient outcomes using the TCGA, further supporting the framework[26–29].

However, a second set of genes was rapidly identified that, despite protecting forks when depleted in BRCA cancers, nevertheless did not confer chemoresistance and appeared to be inconsistent with the dogma; moreover, these genes also did not accurately predict BRCA cancer patient outcomes in the TCGA[30–33]. Several of these proteins, including the fork remodeler SMARCAL1, were thought to stabilize the fork in a reversed structure that was protected from degradation by MRE11, yet no resistance was conferred. Moreover, even inhibiting MRE11, the protein directly implicated in degrading and collapsing forks, was also not reported to confer chemoresistance. These observations were handled by adding additional complexity to the dogma to ensure it agreed with experiment: for example, multiple types of stabilized forks, of which only a subset confer chemoresistance, to explain why protected forks did not always predict poor patient outcomes.

However, the most impactful question had been overlooked: *What if these results indicate the double strand break model is wrong?*

A Complex Process? Or Fundamentally Flawed?

Indeed, if these complexities instead indicated that the fork premise of the dogma was incorrect, then how could double strand breaks be generated from DNA lesions such as crosslinks? Consequently, even the foundation of the dogma - the double strand break - would have to be questioned. Had any complexity been added to the double strand break idea of the dogma to resolve inconsistencies that might indicate a flaw?

A critical examination of the literature revealed this was indeed the case, with the most compelling evidence coming from a patient with Fanconi Anemia, a DNA metabolism disorder that displays developmental defects, genomic instability, and hypersensitivity to genotoxins comparable to that observed for BRCAness. Incredibly, despite a clear diagnosis of Fanconi Anemia with confirmed hypersensitivity to genotoxins, the patient's cells nevertheless were found to have *intact* double strand break repair by homologous recombination using the best experimental methods available[34] - a truly staggering result. Again, although these observations can legitimately be fit to the framework of the dogma by adding complexity - for example, a latent and undetectable defect in double strand break repair; or a subtle defect in repairing just a subset of DNA lesions - the clarity of the conflict between patient and dogma *represents an important opportunity*

and, we propose, demands that other competing frameworks for *BRCAness* be evaluated.

A Competing Framework: The ssDNA Theory of BRCAness and Genotoxic Agents

It is into this context that the ssDNA theory emerged. We had been investigating the different fork protection factors in *BRCAness*, aiming to understand why some of these genes conferred chemoresistance whereas others did not. Our approach was to employ DNA fiber assays, but with a lower dose and time of genotoxin exposure in order to monitor the earliest possible changes to the DNA replication fork, a technique previously described to have detected ssDNA in BRCAness cells[38]. Indeed, we observed ssDNA accurately predicted hypersensitivity in all fork protection systems tested; moreover, our subsequent experiments revealed ssDNA accurately predicted hypersensitivity across a broad range of genetic systems, including known cases and new cases. Critically, ssDNA also accurately predicted hypersensitivity, without added complexity, even in the edge cases that had required modification of the double strand break dogma to remain consistent with experiment (*Table 1*)[39].

This predictive power implicated ssDNA as a fundamental lesion for BRCAness, genotoxins, and hypersensitivity, but the overall role was still unclear. Indeed, ssDNA could in fact be fit onto the existing double strand break dogma - for example, was ssDNA at a fork simply the precursor lesion that would ultimately become the DNA double strand break that causes hypersensitivity? On the other hand, if ssDNA were the

fundamental lesion, and the double strand break dogma were instead incorrect, *how could we differentiate between these two frameworks?*

Cell line	HR	FP	GS	Therapy Response	Case Type
BRCA1/2 deficient	-	-	-	Hypersensitive	Known
BRCA1/2 proficient	+	+	+	Resistant	Known
BRCA2 and CHD4 deficient	-	+	+	Resistant	Known
BRCA2 deficient and EZH2i	-	+	+	Resistant	Known
BRCA2 and FEN1 deficient	-	+	+	Resistant	Known
BRCA2 and ZFHX3 deficient			+	Resistant	New
BRCA1 deficient PDX, hypersensitive			-	Hypersensitive	New
BRCA1 deficient PDX, resistant			+	Resistant	New
BRCA2 deficient and MRE11i	-	+	-	Hypersensitive	Edge
BRCA2 and SMARCAL1 deficient	-	+	-	Hypersensitive	Edge
RAD51 T131P mutant	+	-	-	Hypersensitive	Edge
RAD51 T131P mutant and RADX deficient	+	+	-	Hypersensitive	Edge

Table 1.1: Prediction table demonstrates that ssDNA replication gaps accurately predict chemoresponse in known, new, and edge cases without adding complexity. HR is homologous recombination, FP is fork protection, GS is gap suppression. Cells with GS do not generate ssDNA behind the replication fork. Blank indicates untested. Edge cases are observations that required adding complexity to the dogma to resolve.

A Surprising Prediction is Confirmed: Apoptosis Generates all Detectable DSBs

Historically, confidence in competing models has been determined by developing and testing surprising, specific predictions that would clearly favor one framework over the other[40]. Here, we decided to test what we determined to be the most surprising prediction of a ssDNA worldview - that the double strand breaks were not directly caused by the genotoxic agents, but instead were experimental artifacts created by the programmed cell death machinery.

Indeed, in constructing the previous dogma, apoptosis had initially been considered as the source of the double strand breaks because genotoxins elicit toxicity via

programmed cell death, but was ultimately dismissed because the understanding of apoptosis was incomplete at the time. For example, it is now appreciated that apoptosis causes an ordered - not random - degradation of DNA that results in initial fragments of 100-500kb in size that are subsequently degraded further[41,42]: importantly, this fragmentation pattern appears essentially identical to the fragmentation observed after genotoxic therapy, which can appear within an hour depending on treatment dose. In addition, a role for apoptosis had also been unfavored because double strand breaks were observed after genotoxic treatment in *e. coli*[14,15], which were not thought to have an apoptotic pathway until recently[43–45]. Finally, several covalent inhibitors of apoptosis - called pan-caspase inhibitors - have now been developed that can be used to block all known features of apoptosis, including apoptotic double strand breaks; we therefore employed these agents as controls to isolate the double strand breaks caused directly by genotoxins[46,47].

Strikingly, we observed with pulsed field capillary electrophoresis that all detectable double strand breaks were eliminated by the apoptotic inhibitors - none had been directly created by the genotoxins[39]. Moreover, a critical review of prior literature found corroboration of this phenomenon from apoptotic studies with pulsed field gels, further increasing our confidence in the result[48]. As discussed in our paper that reports this work[39], we considered a number of ways to try to rescue the dogma, but found it impossible to reconcile how an undetectable level of double strand breaks from genotoxins could reasonably be responsible for BRCAness and hypersensitivity. Specifically, apoptotic double strand breaks were already reported to be dispensable for

toxicity; their suppression was not reported to confer resistance[41,42]. Moreover, BRCAness cells maintain backup pathways that should be able to repair and prevent hypersensitivity even if double strand breaks were created at undetectable levels[49]. Importantly, although these backups are error prone, chromosomal instability also did not appear to be a source of hypersensitivity[24,39], further undermining confidence in the dogma and increasing our confidence in an ssDNA framework.

An ssDNA Future?

We propose this body of work leads to high confidence in the ssDNA theory of BRCAness and to an overturn of the double strand break dogma. The apoptotic nature of the observed double strand breaks alone appears to place the dogma in a nearly untenable position[48], and is also undermined by the observation of a hypersensitive Fanconi Anemia patient with intact double strand break repair via homologous recombination[34]. Simultaneously, the dogma now faces competition from an ssDNA theory that is also based in BRCA protein function, fits the observed results with less complexity, and accurately predicts that the observed double strand breaks are apoptotic[39]; these results meet the requirements for a competing theory, and shift confidence away from the dogma and toward the ssDNA framework.

An important test of this new framework will be to determine if ssDNA can be used to identify and generate superior personalized treatments for BRCAness in the future. Indeed, the BRCAness phenotype has been a critical proving ground for personalized

medicine, leading to the development of drugs that specifically kill BRCAness cells, for example by inhibiting PARP1 as highlighted previously; importantly, PARPi are lethal in cells that display BRCAness, but are well tolerated in normal cells, leading to a superior therapeutic window compared to the previous generation of genotoxins[21–23]. As expected, we find inhibition of PARP1 induces ssDNA gaps as consistent with the predictions of our framework, further supporting ssDNA as the targetable defect for BRCAness[50]. Moreover, the success of PARPi is widespread - suggesting that BRCAness is also widespread - and that agents targeting ssDNA could be widely applicable as personalized therapy across cancer types. Importantly, PARPi have been observed to be effective in the general population of breast and ovarian cancers, as well as prostate cancers - even those without specific mutations in the BRCA genes - indicating that the BRCAness phenotype and a likely ssDNA vulnerability is common across cancer types and is caused by a growing list of mutations in DNA metabolism type genes[51–54].

In addition to new drug targets and biomarkers for personalized medicine, several opportunities are unique to the ssDNA framework and are worth highlighting here. First is the potential to develop adjuvant drugs against gap filling and fork restraint, either to prevent the emergence of resistance or to resensitize refractory disease. Indeed, gap filling in particular appears to be a unique cancer adaptation and may therefore be uniquely targeted; several observations implicate the gap filling process known as translesion synthesis as a possible mechanism, and inhibitors are now emerging for clinical use[55]. In addition, a generalizable mechanism of repriming replication is also a

promising target[56]. Moreover, beyond protein biomarkers, it may even be possible to diagnose patients with a BRCAness cancer via DNA combing and atomic force microscopy[57–59], which can observe ssDNA in the genome directly, rather than by relying on a complex genetic profile.

More broadly, evidence indicates ssDNA gaps underline the hypersensitivity of other DNA metabolism disorders, including Fanconi Anemia as described in our manuscript; indeed, both BRCA1 and BRCA2 are reported Fanconi genes[60,61]. Moreover, recent reports also suggest ssDNA gaps are a source of mutations that result even from normal cellular metabolism in BRCAness cells[62], raising the distinct possibility ssDNA is fundamental to genomic instability. In addition, ssDNA could even underlie cell failure in DNA metabolism based diseases[63] as well as cancer initiation and the BRCA haploinsuffiency phenotype[64]. Critically, it may be possible to treat DNA metabolism disorders, and also to prevent cancer initiation, by suppressing ssDNA; homologous recombination, in addition to a role in double strand break repair, may also have a key role in the resolution of such ssDNA lesions that could possibly be restored in BRCAness backgrounds. Accordingly, we propose it will be essential to evaluate the therapeutic potential of the ssDNA theory for BRCAness and DNA metabolism disorders and to encourage further competition between the frameworks.

CHAPTER II: RESULTS

Replication Gaps Underlie BRCA-deficiency and Therapy Response

This chapter is published as a featured article in *Cancer Research.* The citation for the paper and *Research Highlight*, as well as the published author contributions, are listed below. N. J. Panzarino performed all experiments except for the patient derived xenografts reported in Figures 2.4 and 2.5.

1. Panzarino, N. J. *et al.* Replication Gaps Underlie BRCA Deficiency and Therapy Response. *Cancer Research.* 2021.
2. Canman, C. Which Holds the Key to BRCAness: Inability to Repair the Break, Protect the Fork, or Prevent the Gap? *Cancer Research.* 2021.

Abstract

Defects in DNA repair and the protection of stalled DNA replication forks are thought to underlie the chemosensitivity of tumors deficient in the hereditary breast cancer genes BRCA1 and BRCA2 (BRCA). Challenging this assumption are recent findings that indicate chemotherapies such as cisplatin used to treat BRCA-deficient tumors do not initially cause DNA double-strand-breaks (DSB). Here we show that single-stranded DNA (ssDNA) replication gaps underlie the hypersensitivity of BRCA-deficient cancer and that defects in homologous recombination (HR) or fork protection (FP) do not. In BRCA-deficient cells, ssDNA gaps developed because replication was not effectively restrained in response to stress. Gap suppression by either restoration of fork restraint or gap filling conferred therapy resistance in tissue culture and BRCA patient tumors. In contrast, restored FP and HR could be uncoupled from therapy resistance when gaps were present. Moreover, DSB were not detected after therapy when apoptosis was inhibited, supporting a framework in which DSB are not directly induced by genotoxic agents, but rather are induced from cell death nucleases and are not fundamental to the mechanism of action of genotoxic agents. Together, these data indicate that ssDNA replication gaps underlie the BRCA cancer phenotype, "BRCAness," and we propose they are fundamental to the mechanism-of-action of genotoxic chemotherapies.

Statement of Significance

This study suggests that ssDNA replication gaps are fundamental to the toxicity of genotoxic agents and underlie the BRCA-cancer phenotype "BRCAness," yielding promising biomarkers, targets, and opportunities to re-sensitize refractory disease.

Introduction

Mutations in the hereditary breast cancer genes, BRCA1 and BRCA2, first demonstrated that cancer is a genetic disease in which susceptibility to cancer could be inherited (1). In addition to breast cancer, mutated BRCA1 or BRCA2 cause a predisposition to other cancer types, including ovarian, pancreatic, and colorectal cancers. Importantly, cancers with mutated BRCA genes are hypersensitive to cisplatin, a first-line anti-cancer chemotherapy that has been the standard of care for ovarian cancer for over 40 years (2). BRCA-deficient cancers are thought to be hypersensitive to cisplatin due to their inability to repair cisplatin-induced DNA double strand breaks (DSBs) by homologous recombination (HR) (3). Accordingly, it is proposed that the DSBs are created when replication forks collide with the cisplatin-DNA crosslinks, causing the fork to collapse into DSBs (4). This broken-fork-model was further supported by reports that mutations in the BRCA genes also lead to defective fork protection (FP), which is thought to render forks vulnerable to fork collapse and subsequent double strand break induction (5-7). Correspondingly, chemoresistance in BRCA cancer is proposed to occur when either HR or FP is restored, with the latter

largely preventing DSBs and therefore eliminating the requirement for HR. Importantly, this hypersensitivity phenotype is known as BRCAness and is thought to arise in a range of cancers via mutations in genes that function similar to BRCA1 and BRCA2 in DSB repair.

However, recent findings challenge the fundamental premise that DSBs are the critical lesion for cisplatin sensitivity. Notably, DNA crosslinks do not appear to initially cause replication forks to collapse and can be bypassed (8, 9). Moreover, in the majority of genetic models currently reported, restored FP fails to restore cisplatin resistance, suggesting the cisplatin lesions do not collapse forks, and therefore calls into question how cisplatin crosslinks could be converted into DSBs (4, 10). Most saliently, indicating that the fundamental sensitizing lesion may in fact not be a DSB, reports indicate even HR proficient cells can nevertheless display hypersensitivity to cisplatin and other genotoxic agents (11-13). Moreover, in addition to cisplatin, BRCA-deficient cells and patient tumors have recently been found to be hypersensitive to a wide range of genotoxic agents that were previously thought to be mechanistically distinct, including doxorubicin, Poly(ADP-ribose) polymerase 1 inhibition (PARPi), and other first-line agents, even including the platinum analog oxaliplatin, which is not thought to generate DSBs (14). Moreover, recent reports indicate that cisplatin toxicity in triple negative breast cancer is unrelated to loss of DNA repair factors (15). Taken together, these findings indicate an opportunity to revise the current framework for both BRCAness as well as the mechanism-of-action of first-line genotoxic chemotherapies.

Here, we propose a model for genotoxic chemotherapy in which hypersensitivity derives from single stranded DNA (ssDNA) formation, and not from the failure to repair or prevent the induction of DSBs due to defects in HR or FP. Specifically, we observed in hypersensitive BRCA-deficient cells that ssDNA gaps develop because DNA replication is not effectively restrained in response to genotoxic stress. Moreover, we observed ssDNA gaps could be suppressed by either restored fork restraint or by gap filling, both of which conferred resistance to genotoxic therapy in tissue culture and BRCA patient tumors. In contrast, we observed that cells with proficient HR and FP are nevertheless hypersensitive to chemotherapy if ssDNA gaps remain. Finally, we find that when apoptosis is inhibited, DSBs are no longer detectable after therapy, suggesting that DSBs are instead created by the programmed cell death nucleolytic machinery and that ssDNA gaps are the critical lesion that determines therapy response. Accordingly, we propose that ssDNA replication gaps underlie the BRCA cancer phenotype, “BRCAness,” and are fundamental to the mechanism-of-action of genotoxic chemotherapies.

Results

To analyze the mechanism underlying the hypersensitivity of BRCA-deficient cancers to chemotherapy, we monitored the immediate response of DNA replication forks to replication stress with DNA fiber assays. Following the incorporation of nucleotide analogs into nascent DNA as the cells replicate in the presence or absence of stress, the progression of replication forks was detected by immunofluorescence. Specifically,

we measured the lengths of the labeled DNA when the cells were exposed to 0.5mM hydroxyurea (HU), a dose that induces replication stress without fully depleting nucleotide pools (17). The condition yields high quality DNA fibers and has been used as a model to study fork responses to genotoxic therapy such as cisplatin, which yields lower quality fibers because cisplatin covalently damages DNA (17, 18). We compared the parental PEO1 cancer cell line, which expresses a truncated BRCA2 protein and is hypersensitive to cisplatin, to the BRCA2 proficient PEO1 reversion cell line, C4-2, which expresses a full-length BRCA2 protein and is resistant to cisplatin (19) (Figure 2.1A). Both cell lines were incubated with the DNA analog 5-Iodo-2′- deoxyuridine (IdU) for thirty minutes as an internal control to label regions of active replication, followed by the DNA analog 5-chloro-2′-deoxyuridine (CldU) for two hours in the presence of 0.5mM HU in order to monitor the immediate response of DNA replication to genotoxic stress. An additional set of cells were exposed to CldU without HU to serve as untreated controls.

We observed that the BRCA2-deficient PEO1 cells failed to fully restrain replication in response to HU when compared to the BRCA2-proficient C4-2 cells, as indicated by the longer CldU tracks observed in PEO1 compared to C4-2 (Figure 2.1B). As expected, both untreated controls displayed substantially longer CldU tracks than either of the HU treated cells (Figure 2.2A, B), therefore indicating that replication is restrained after stress, and that this restraint is less effective in BRCA2 deficient cells. Moreover, we observed similar replication-restraint defects in other BRCA-deficient cells that are hypersensitive to cisplatin, including the BRCA2 deficient Chinese hamster cell line VC-

8 (6), BRCA2 depleted C4-2 cells, and BRCA1 deficient breast cancer lines (HCC1937 and MDA-MB-436) (Figure 2.2C-H). We also observed that the replication restraint defects were not exclusive to HU, but also detected following cisplatin (Figure 2.2I). In agreement with the DNA fiber assays, analysis of global cellular DNA replication based on incorporation of the analog 5-Ethynyl-2´-deoxyuridine (EdU) similarly indicated that BRCA2 deficient cells failed to properly restrain DNA replication during stress (Figure 2.1C).

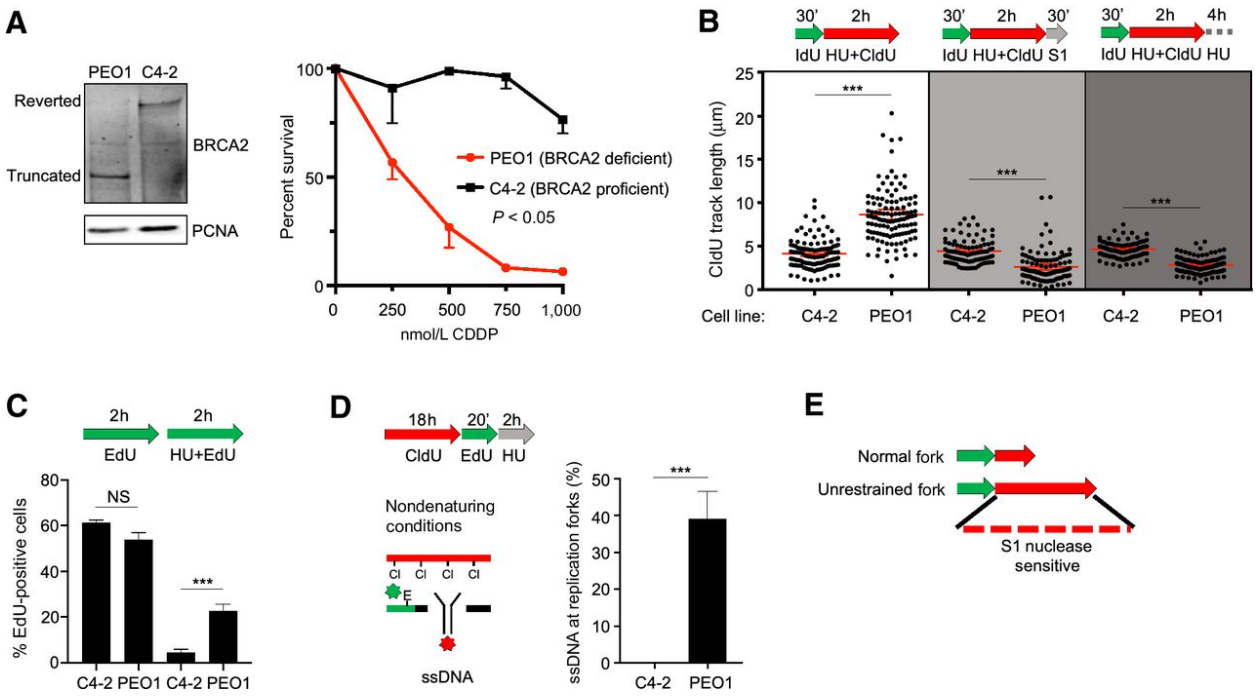

Figure 2.1: BRCA2-deficient cancer cells fail to restrain replication in the presence of stress, generating regions of ssDNA gaps that are destroyed after continued exposure. A, Western blot analysis detects truncated BRCA2 protein in BRCA2-deficient PEO1 cells and detects full-length BRCA2 protein in BRCA2-proficient C4-2 cells that are derived from PEO1 cells (left). Cell survival assay confirms PEO1 cells are hypersensitive to cisplatin compared with C4-2 cells (right). B, Schematic and quantification of CldU track length (white) shows that PEO1 cells fail to arrest replication in the presence of stress. These regions are degraded by S1 nuclease (light gray) and are also destroyed after continuous exposure to replication stress (dark gray). Each dot represents one fiber. Experiments were performed in biological triplicate with at least 100 fibers per replicate. Statistical analysis according to two-tailed Mann–Whitney test; ***, $P < 0.001$. Mean and 95% confidence intervals are shown. C,Schematic and quantification of nuclear imaging identifies a greater percentage of EdU-positive cells in PEO1 as compared with C4-2. *, $P < 0.05$ as determined by *t* test of biological triplicate experiments. D, Nondenaturing fiber assay identifies exposed ssDNA adjacent to newly replicating regions after stress in PEO1, but not C4-2 cells. Regions of active replication were detected with EdU Click chemistry. ***, $P < 0.01$ as determined by *t* test of biological triplicate experiments. E, Model of fiber assay interpretation. NS, not significant.

Figure S1

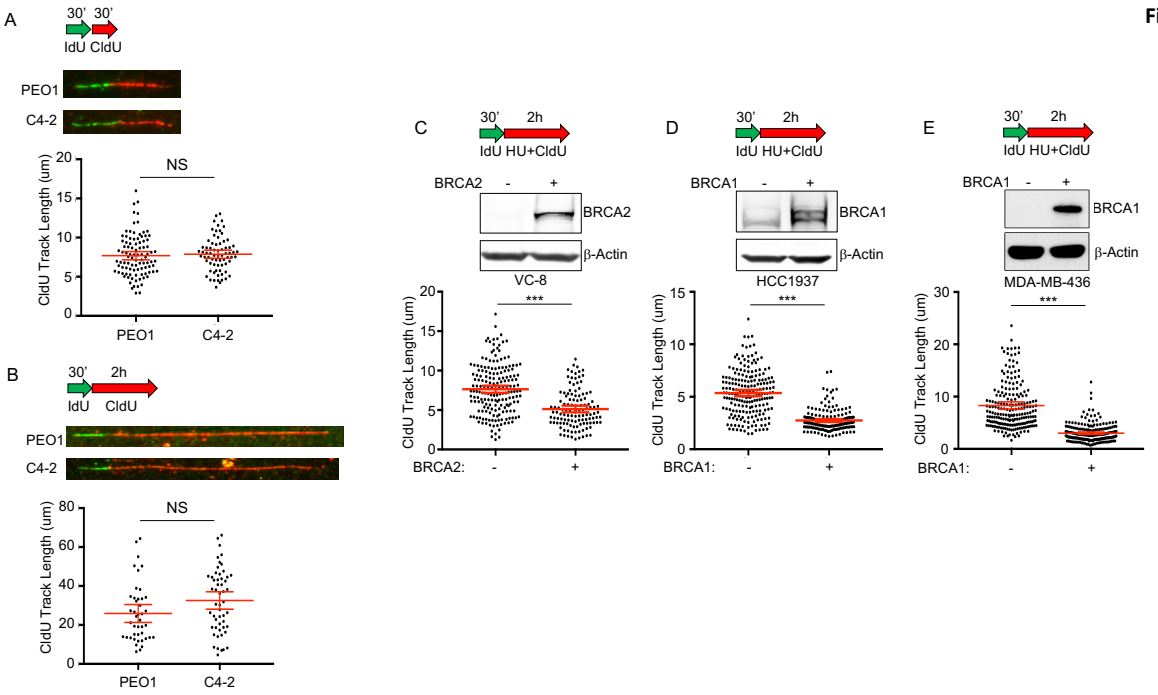

Figure S1 Continued

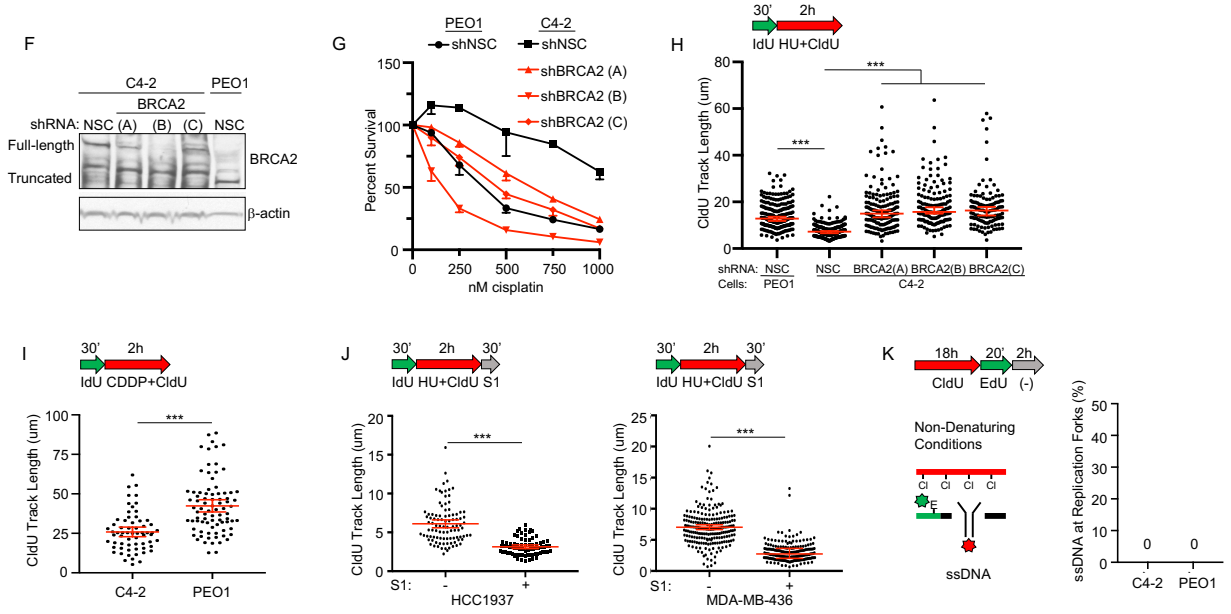

Figure 2.2: BRCA-deficient cancer cells fail to restrain replication in the presence of stress and ssDNA gaps develop. A) Schematic, representative images, and quantification of CldU track length shows that PEO1 and C4-2 have similar track lengths in untreated conditions. B) Same as A, but with a 2h pulse. C) Western blot confirms BRCA deficiency and complementation in BRCA2 deficient VC-8 hamster cells and in the BRCA1 deficient breast cancer cells D) (HCC1937) and E) (MDA-MB-436). Schematic (above) and quantification of CldU track length shows BRCA complementation restores fork restraint. F) Western blot confirms BRCA2 is depleted in C4-2 by three distinct shRNA reagents. G) Cell survival assay confirms C4-2 cells with BRCA2 depleted are hypersensitive to cisplatin compared to C4-2-shNSC cells (with PEO1-shNSC as a hypersensitivity control). H) Schematic (above) and quantification of CldU track length by dynamic molecular combing shows BRCA2 depletion in BRCA2-proficient C4-2 creates a defect in slowing replication in response to HU as observed for BRCA2-deficient PEO1 cells. I) Schematic and quantification of

CldU track length by dynamic molecular combing shows BRCA2 deficient PEO1 cells fail to effectively arrest replication in response to 1000nM CDDP compared to BRCA2 proficient C4-2 cells. J) Schematic and quantification of CldU track length shows BRCA1 deficient HCC1937 (top) and MDA-MB-436 (bottom) are sensitive to S1 nuclease. Each dot represents one fiber. Experiments were performed in biological duplicate with at least 100 fibers per replicate. Statistical analysis according to two-tailed Mann-Whitney test; $p < 0.001$ (***). Mean and 95% confidence intervals are shown. K) Nondenaturing fiber assay does not detect ssDNA in untreated BRCA2 deficient PEO1 or C4-2 cells as a control.

We hypothesized that failure to fully restrain replication during stress in BRCA-deficient cells would result in poorly replicated regions that contain ssDNA. To test this hypothesis, we performed the DNA fiber assay followed by incubation with S1 nuclease. S1 cuts at ssDNA regions and secondary DNA structures, but does not cut dsDNA (20). Indeed, labelled nascent DNA tracks were S1 sensitive in BRCA2-deficient PEO1 cells, but not in the BRCA2-proficient C4-2 cells (Figure 2.1B). These S1 sensitive nascent DNA regions were also degraded after continued exposure to replication stress, indicating that nascent DNA in regions behind the fork are degraded under continued stress (Figure 2.1B). Similar to BRCA2, BRCA1 deficient cancer cells (HCC1937 and MDA-MB-436) also displayed DNA replication tracks that were sensitive to S1 nuclease after treatment with HU (Figure 2.2J). In addition, we employed a non-denaturing DNA fiber assay that detects ssDNA in regions of active DNA replication and confirmed that following HU, ssDNA (detectable by the CldU antibody only in exposed ssDNA regions) was present adjacent to newly replicating regions (detected as EdU signal) in the BRCA2 deficient PEO1 cells, but not in the BRCA2 proficient C4-2 cells (Figure 2.1D). In contrast, ssDNA was not detected in the untreated cells (Figure 2.2K). Thus, BRCA-deficient cancer cells fail to fully restrain replication in the presence of stress, creating ssDNA regions (Figure 2.1E) that are degraded after additional exposure to stress.

We hypothesized that ssDNA gaps confer chemosensitivity in BRCA cancer, and that mechanisms of chemoresistance would suppress these gaps. Indeed, we previously

found that depletion of the chromatin remodeling enzyme CHD4 confers cisplatin resistance in BRCA2 deficient PEO1 cells (Figure 2.3A) (21). Therefore, we tested if CHD4 depletion would reduce ssDNA gaps in PEO1 cells in the S1 fiber assay. When CHD4 was depleted, we observed protection from S1 nuclease after HU compared to the PEO1 non-silencing control, which was degraded to a length below even the arrested forks found in BRCA2 proficient C4-2 cells, therefore indicating ssDNA gaps were reduced in the resistant cells after HU treatment (Figure 2.3B, Figure 2.4A-D). Moreover, when CHD4 was depleted, we found nascent DNA tracks were not degraded after continued exposure to HU (Figure 2.3B). Collectively, these findings indicate that CHD4-depletion in BRCA2 deficient cells reduced ssDNA gaps during replication stress.

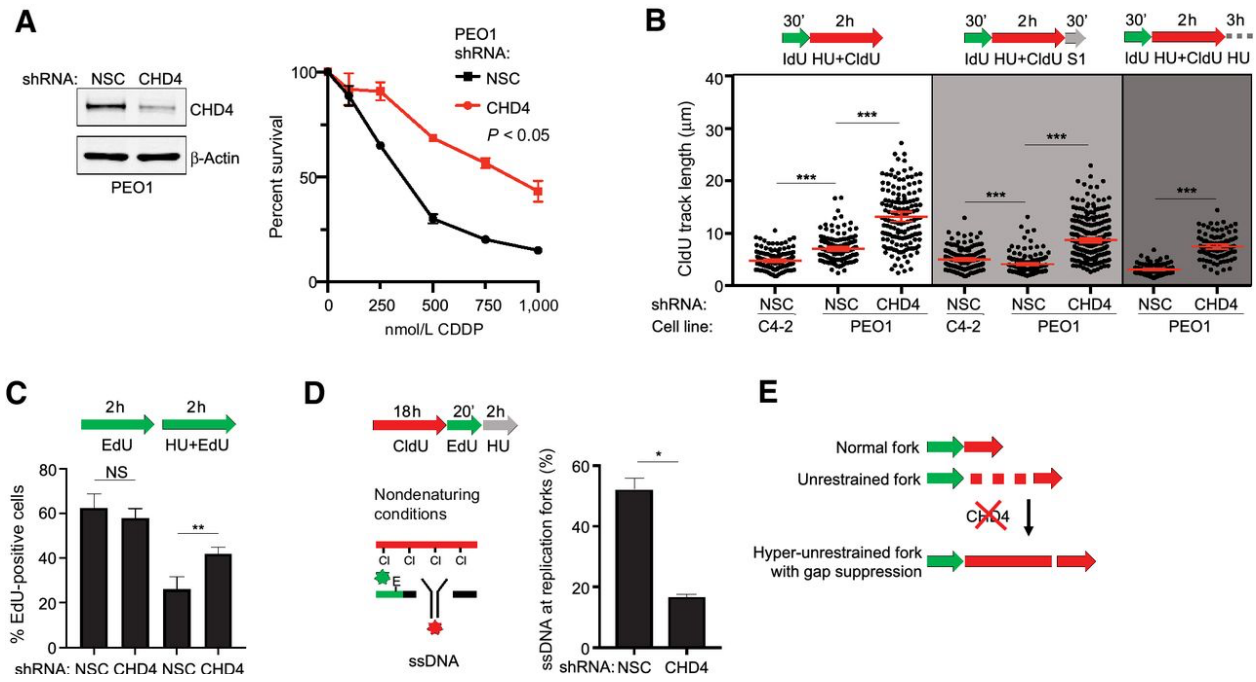

Figure 2.3: CHD4 depletion suppresses ssDNA gaps, but does not restore fork restraint. A, Western blot analysis confirms CHD4 is depleted by short hairpin RNA (shRNA) compared with nonsilencing control (NSC) in BRCA2-deficient PEO1 cells (left). Cell survival assay confirms PEO1 cells with depleted CHD4 are resistant to cisplatin compared with PEO1 NSC (right). B,Schematic and quantification of CldU track length shows that PEO1 cells with depleted CHD4 increase replication in the presence of stress (white). These regions are protected from S1 nuclease (light gray) and are also protected after continuous exposure to replication stress (dark gray). Each dot represents

one fiber. Experiments were performed in biological triplicate with at least 100 fibers per replicate. Statistical analysis according to two-tailed Mann–Whitney test; ***, $P < 0.001$. Mean and 95% confidence intervals are shown. C, Schematic and quantification of nuclear imaging identifies a greater percentage of EdU-positive cells in CHD4-depleted PEO1 cells as compared with NSC. **, $P < 0.01$ as determined by *t* test of biological triplicate experiments. D, Nondenaturing fiber assay identifies ssDNA adjacent to newly replicated regions after stress is reduced when CHD4 is depleted in PEO1 cells. Regions of active replication were detected with EdU Click chemistry. *, $P < 0.05$ as determined by *t* test of biological duplicate experiments. E, Model of fiber assay interpretation. NS, not significant.

Figure S2

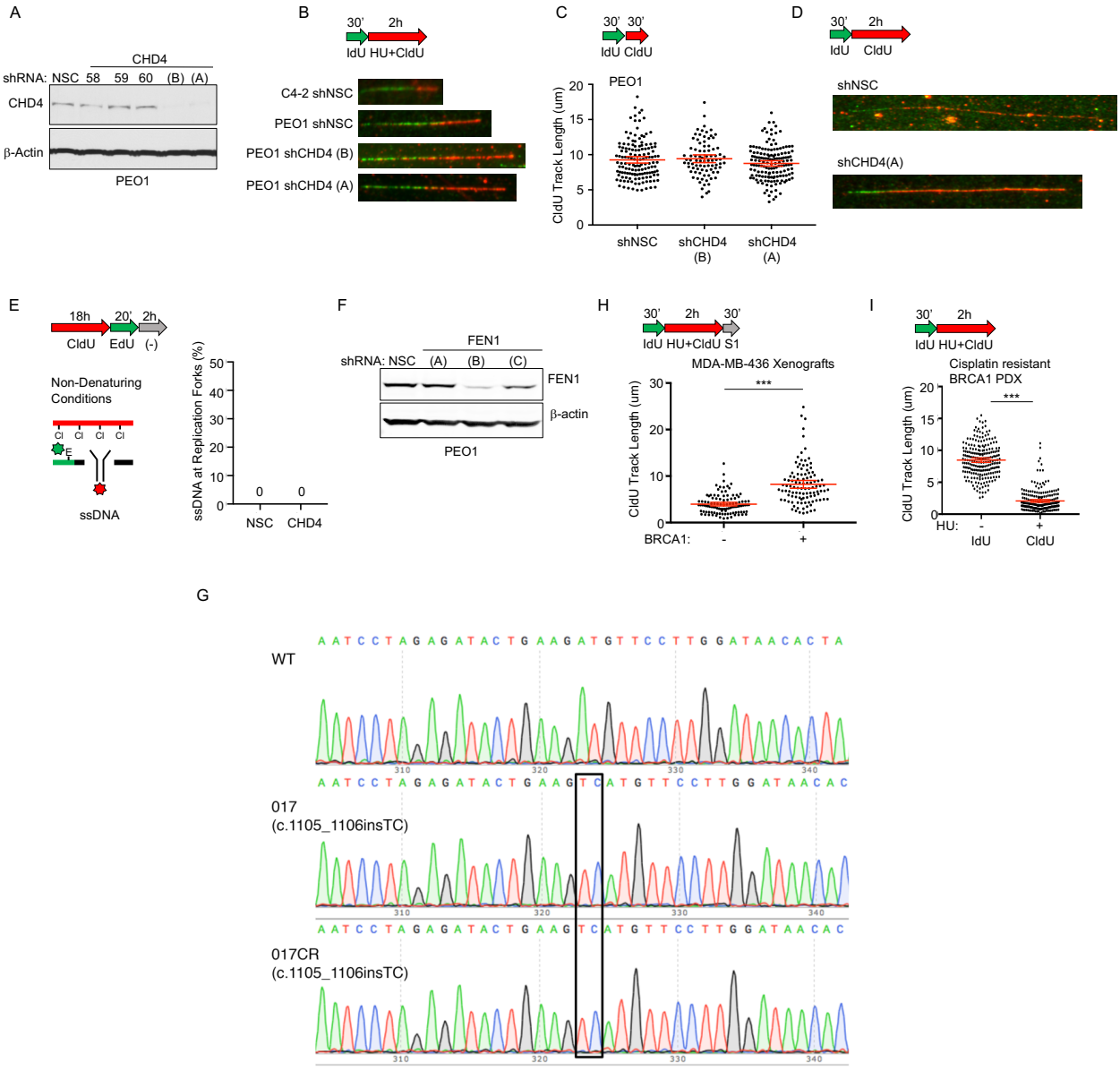

Figure 2.4: Replication restraint, depletion, and PDX controls. A) Western blot confirms CHD4 is depleted by shRNA(A) and shRNA(B) compared to non-silencing control (NSC) in BRCA2 deficient PEO1. B) Schematic and representative images of CldU track length shows that CHD4 depletion increases replication in the presence of stress. See Figure 2.3B and 2.7E for track lengths quantification for shRNA(A) and shRNA(B), respectively. C)

Schematic and representative images show that CHD4 shRNA and NSC have similar track lengths in unchallenged conditions with thirty minute labeling or D) two hour labeling. E) Nondenaturing fiber assay does not detect ssDNA in untreated BRCA2 deficient PEO1 with either CHD4 depleted or non-silencing control (NSC). F) Western blot of shRNA confirms FEN1 is depleted by shRNA (Hairpins A and B; B selected for experiments) compared to non-silencing control (NSC) in BRCA2 deficient PEO1. G) DNA sequencing of Wild Type BRCA1, the initial hypersensitive patient derived xenograft, and the resulting cisplatin resistant patient derived xenograft. H) Schematic and quantification of CIdU track length in MDA-MB-436 xenografts shows that complementation with BRCA1 protects from S1 nuclease. I) Schematic and quantification of DNA track length shows replication is efficiently arrested in BRCA1 deficient patient derived xenografts that have acquired chemoresistance. Each dot represents one fiber. Experiments were performed in biological duplicate with at least 100 fibers per replicate. Statistical analysis according to two-tailed Mann-Whitney test; $p < 0.001$ (***). Mean and 95% confidence intervals are shown.

Notably, however, replication restraint in response to stress was not observed upon CHD4 depletion. Instead, the replication tracks during HU appeared to be longer in CHD4-depleted PEO1 cells compared to PEO1 control cells (Figure 2.3B, Figure 2.4B, C, D). Moreover, in agreement with the fiber assays, analysis of global cellular replication by EdU incorporation demonstrated that CHD4-depleted PEO1 cells increased replication after HU treatment as compared to PEO1 or C4-2 control cells (Figure 2.3C). In addition, we also observed a significant reduction in ssDNA adjacent to regions of active replication in the non-denaturing DNA fiber assay (Figure 2.3D, Figure 2.4E). Thus, ssDNA gap formation was suppressed in chemoresistant BRCA2 deficient cells with CHD4-depletion, but fork restraint was not restored (Figure 2.3E). Taken together, these data indicate that chemoresistant cells display either restored fork restraint, as observed in the BRCA2 reversion cell line C4-2, or continuous replication without ssDNA gap formation, as in the CHD4-depleted PEO1 cells (Figure 2.3E).

Our data indicate that suppression of ssDNA replication gaps in BRCA-deficient cancer could confer chemoresistance. To address this possibility, we sought to identify additional genes similar to CHD4 that confer chemoresistance when depleted in BRCA2 deficient cells, and subsequently determine if gaps were suppressed. Therefore, we

performed quantitative mass spectrometry proteomics to compare the CHD4-interactome in BRCA2 deficient and BRCA2 proficient cells after cisplatin treatment (Figure 2.5A). Indeed, in addition to known CHD4-interactors (22), we also observed that CHD4 interacted with two proteins associated with chemoresistance in BRCA2 deficient cells: EZH2, which confers chemoresistance when inhibited, and FEN1, which confers chemoresistance when depleted, but is synthetic lethal when knocked out (Figure 2.5B) (21, 23-25). In BRCA2 deficient cells, we also found enrichment of the known CHD4-interacting protein ZFHX3 (26) and that ZFHX3 depletion enhanced cisplatin resistance in PEO1 cells (Figure 2.5C). Furthermore, analysis of TCGA patients revealed that low ZFHX3 mRNA levels predicted poor tumor-free survival in ovarian cancer patients with germline BRCA2 deficiency (Figure 2.5D) as previously found for CHD4, EZH2, and FEN1 (21, 23, 24). Strikingly, as found for CHD4-depletion, we observed that depletion of ZFHX3 or FEN1, or inhibition of EZH2, increased replication in BRCA2 deficient cells in the presence of HU, and as shown in the S1 nuclease assay, ssDNA gaps were suppressed (Figure 2.5E, 2.6F). Together, these findings suggest that loss of CHD4, EZH2, FEN1, and ZFHX3 suppress ssDNA gaps during stress to confer chemoresistance.

Next, we tested if ssDNA gaps could predict chemosensitivity and resistance in BRCA patient tumor samples. Specifically, we utilized a triple-negative breast cancer patient-derived xenograft (PDX), PNX0204, from a patient with a hemizygous germline BRCA1 mutation (1105insTC); the wild type BRCA1 allele was lost in the tumor, following a Loss of Heterozygosity model (Figure 2.4G). PNX0204 tumors were originally

hypersensitive to cisplatin treatment. After several rounds of cisplatin treatment and serial passage in mice, resistant tumors developed. The sensitive and resistant tumors were then tested for S1 sensitivity, with PEO1 (Figure 2.5F) and MDA-MB-436 (Figure 2.4H) xenografts serving as controls. After HU, we observed that the DNA fibers of cisplatin-sensitive PDX cells were degraded by S1 nuclease, but the fibers of cisplatin-resistant PDX cells were not, indicating ssDNA gaps had been suppressed in the resistant patient samples (Figure 2.5F). Notably, in resistant PDX, ssDNA gaps were suppressed either by continuous replication (Figure 2.5F), or by restored fork slowing (Figure 2.4I), indicating that loss of ssDNA gaps had occurred in BRCA patient tumors de novo and accurately predicted acquired cisplatin resistance.

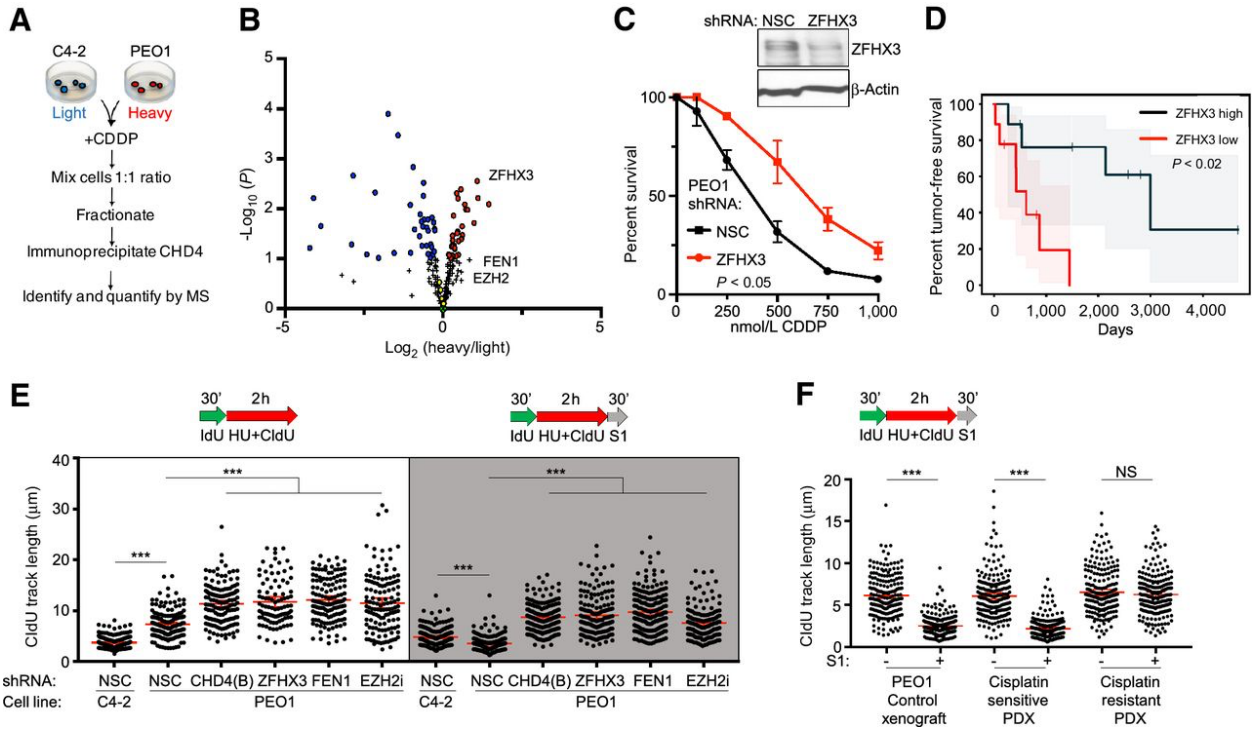

Figure 2.5: Suppression of ssDNA gaps accurately predicts poor therapy response in both cell culture and patient xenografts. A, Overview of the SILAC CHD4 immunoprecipitation experiment. B, SILAC immunoprecipitation reveals that CHD4 interacts with ZFHX3, FEN1, and EZH2 after cisplatin treatment. Red and blue circles are proteins significantly enriched in the CHD4 network of either PEO1 or C4-2 cells. Green (X) represents CHD4. Yellow circles are known CHD4 interacting partners from the NurD complex, including MTA1, HDAC1, MTA2, and HDAC2 (22); ZFHX4 was also identified and is a known CHD4 interacting partner (26). Black plus signs represent proteins not significantly enriched in the CHD4 network of either PEO1 or C4-2. Three biological replicates were performed; see

Materials and Methods for statistical analysis. C, Western blot analysis confirms ZFHX3 is depleted by short hairpin RNA (shRNA) in PEO1 cells as compared with nonsilencing control (NSC). Cell survival assay confirms PEO1 cells with depleted ZFHX3 are resistant to cisplatin compared with PEO1 NSC. D, Reduced ZFHX3 mRNA levels predict poor patient response to therapy (progression-free survival) for patients with ovarian cancer with germline BRCA2 deficiency from TCGA database ($P < 0.02$). Shaded area represents the 95% confidence interval. E,Schematic and quantification of CldU track length shows that depletion of CHD4 [shRNA(B)], ZFHX3, or FEN1, or inhibition of EZH2, increases replication in the presence of stress (white) and protects nascent DNA from S1 nuclease (gray). F, Schematic and quantification of CldU track length shows S1 fiber sensitivity is suppressed in BRCA1-deficient PDXs that have acquired chemoresistance. Each dot represents one fiber. Experiments were performed in biological triplicate with at least 100 fibers per replicate; the xenograft fiber assay was performed in duplicate. Statistical analysis according to two-tailed Mann–Whitney test; ***, $P < 0.001$. Mean and 95% confidence intervals are shown. NS, not significant.

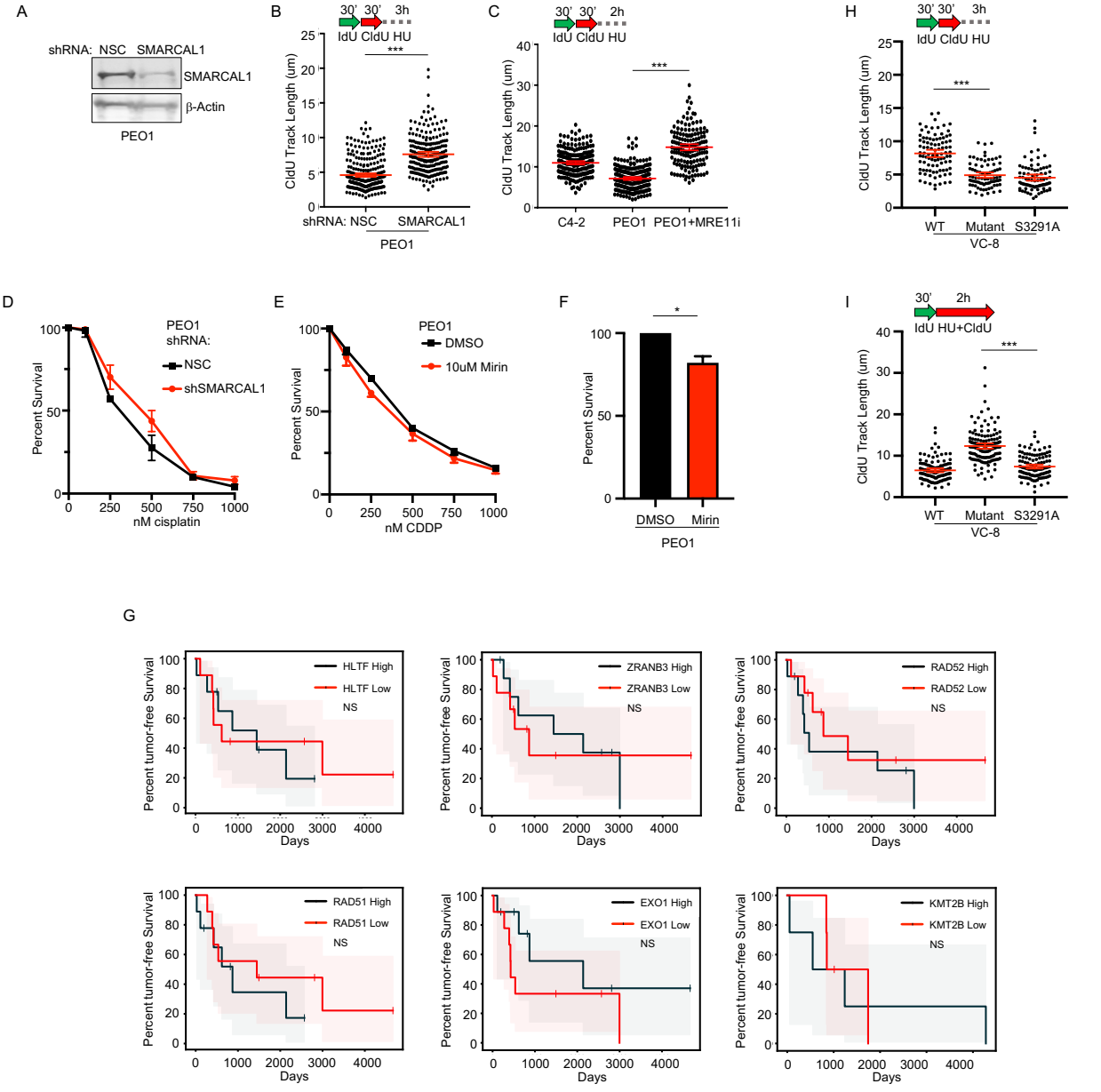

Figure 2.6: Depletion of SMARCAL1 or inhibition of MRE11 restores FP, but do not predict patient response and do not suppress ssDNA gaps, which are distinct from fork degradation. A) Western blot confirms SMARCAL1 is depleted

in BRCA2-deficient PEO1 by shRNA as compared to NSC. B, C) Schematic and quantification of CldU track length shows that PEO1 with depleted SMARCAL1 or inhibited MRE11 protects replication forks after exposure to stress. D) Cell survival assay confirms that SMARCAL1 depletion in PEO1 cells does not confer cisplatin resistance. E) Cell survival assay confirms 10uM MRE11i in PEO1 cells does not confer cisplatin resistance (cisplatin and mirin both given for 18h). F) 18h MRE11i in PEO1 cells reduces viability by approximately 15% after ten days. G) Low mRNA levels of the FP modulators HLTF ($p > 0.30$), ZRANB3 ($p > 0.20$), RAD52 ($p > 0.39$), RAD51 ($p > 0.58$), EXO1 ($p > 0.17$), and KMT2B ($p > 0.72$) fail to accurately predict poor response of ovarian cancer patients with germline BRCA2 deficiency in the TCGA dataset. Shaded area represents the 95% confidence interval. H) Schematic and quantification of CldU track length shows that VC-8 complimented with BRCA2 S3291A are deficient for replication fork protection. I) Schematic and quantification of CldU track length shows that VC-8 complimented with BRCA2 S3291A are proficient for replication fork slowing. Each dot represents one fiber. Experiments were performed in biological duplicate with at least 100 fibers per replicate. Statistical analysis according to two-tailed Mann-Whitney test; $p < 0.001$ (***). Mean and 95% confidence intervals are shown.

These findings present the idea that ssDNA gaps underlie chemosensitivity, and that loss of FP or HR do not. If so, when gaps are present, it should be possible to uncouple FP and HR from therapy response. To test this prediction, we first restored FP by inhibition of MRE11 or depletion of SMARCAL1 in BRCA2-deficient PEO1 cells (6, 27, 28). Nevertheless, even though FP was restored, cisplatin resistance was not conferred and, as predicted by our model, ssDNA gaps remained as demonstrated by S1 nuclease degradation (Figure 2.7A,B and 2.5A-F). Moreover, neither SMARCAL1, nor MRE11 or other reported FP factors, were predictive of BRCA2 cancer patient response based on mRNA levels in the TCGA database (Figure 2.7C and 2.6G), suggesting that ssDNA gaps, but not FP, determines therapy response.

Additionally, we tested if ssDNA gaps were distinct from fork degradation. Specifically, we analyzed gaps in VC-8 cells that express either wild-type BRCA2 or a BRCA2 mutant version (S3291A) that is deficient for FP yet resistant to chemotherapy (6). We did not detect ssDNA gaps in the S3291A cells, thereby confirming that fork degradation can occur without the accumulation of ssDNA gaps (Figure 2.6H,I) and that BRCA function in ssDNA gap suppression is distinct from FP.

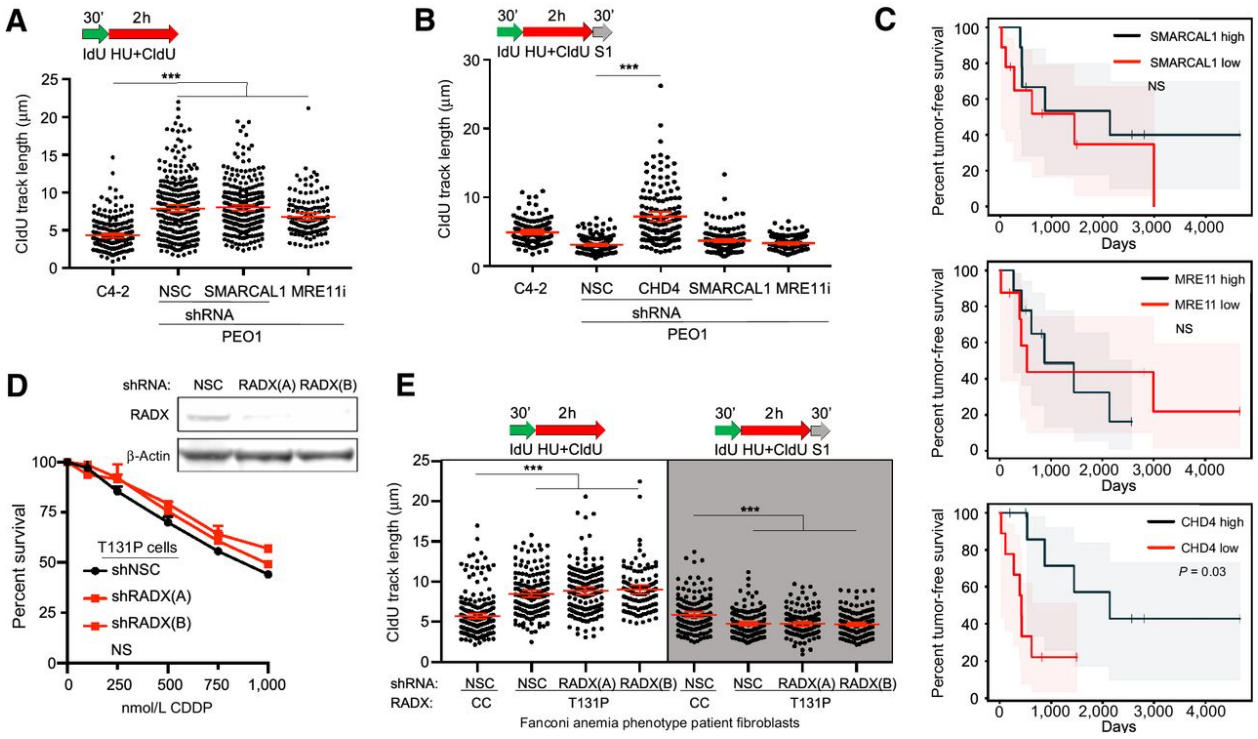

Figure 2.7: ssDNA replication gaps, and not FP or HR, determine patient response to chemotherapy. A and B, Schematic and quantification of CldU track length in PEO1 cells shows that depleted SMARCAL1 or inhibited MRE11 does not increase replication in the presence of stress (A) and does not protect from S1 nuclease, unlike CHD4 depletion (B). C, Neither SMARCAL1 nor MRE11 mRNA levels predict response of patients with ovarian cancer with germline BRCA2 deficiency in TCGA dataset (P > 0.8 and P > 0.5, respectively). In contrast, CHD4 mRNA levels do predict response in these patients (P = 0.03). Shaded area represents the 95% confidence interval. D, Western blot analysis confirms RADX is depleted by two short hairpin RNA (shRNA) reagents in T131P cells compared with nonsilencing control (NSC; top). Cell survival assay confirms RAD51 T131P cells remain hypersensitive to cisplatin even when RADX is depleted (bottom). E, Schematic and quantification of CldU track length (white) shows that fibroblasts from a Fanconi anemia–like patient with a mutant allele of RAD51 (T131P; HR-proficient cells and cisplatin hypersensitive) fail to arrest replication in the presence of stress even when RADX is depleted, and these regions are degraded by S1 nuclease (light gray). WT Fanconi anemia cells were corrected by CRISPR to delete the dominant-negative T131P RAD51 allele. Each dot represents one fiber. Experiments were performed in biological triplicate with at least 100 fibers per replicate. Statistical analysis according to two-tailed Mann–Whitney test; ***, P < 0.001. Mean and 95% confidence intervals are shown. NS, not significant.

We also considered the possibility that our ssDNA gap model could explain a discrepancy in the literature in which cells from a patient with Fanconi Anemia (FA) were sensitive to cisplatin and other genotoxic agents as expected, but were surprisingly found to be proficient in HR (12). Indeed, we found wide-spread ssDNA gap induction in the S1 assay in these FA patient cells; specifically, we observed S1

sensitivity in the FA patient fibroblasts that maintain a RAD51 mutant (T131P) allele as compared to isogenic RAD51 wild type fibroblasts (CRISPR corrected after isolation from the patient) (Figure 2.8A). Importantly, the T131P cells are deficient for FP, but FP can be restored by depletion of the RAD51 negative regulator RADX in T131P (29). However, despite both proficient HR and FP, even the T131P cells with depleted RADX remained cisplatin hypersensitive, and we observed ssDNA gaps remained by S1 assay; importantly, these gaps were eliminated in the wild type (CRISPR corrected) fibroblast control (Figure 2.7D,E, 2.8B). Together, these results suggest that the ssDNA gap model has superior predictive power compared to either the FP or HR models of therapy response and suggests that ssDNA replication gaps are fundamental to the mechanism-of-action of first-line genotoxic chemotherapies.

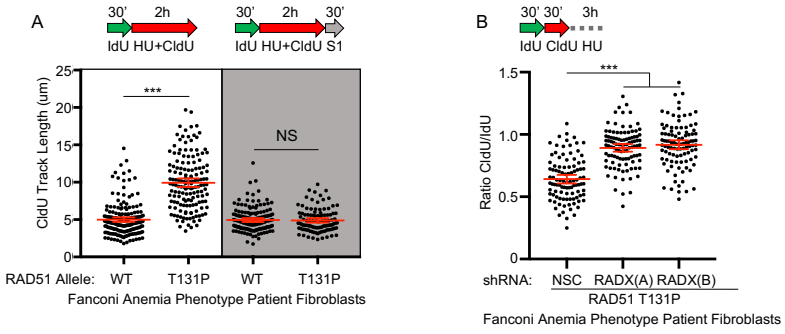

Figure 2.8: Fanconi Anemia Patient Fibroblasts with a RAD51 T131P Mutant Allele (HR Proficient, FP Deficient) Generate ssDNA Gaps, and FP is restored by RADX depletion. A) Schematic and quantification of CldU track length shows (white panel) that RAD51 T131P cells fail to arrest replication in the presence of stress compared to the CRISPR corrected control that deletes the dominant T131P allele. These regions are degraded by S1 nuclease (light grey panel). B) Schematic and quantification of CldU track length shows that RAD51 T131P cells are FP deficient, and depletion of RADX confers FP. Each dot represents one fiber. Experiments were performed in biological triplicate with at least 100 fibers per replicate. Statistical analysis according to two-tailed Mann-Whitney test; $p < 0.001$ (***). Mean and 95% confidence intervals are shown.

We next tested a surprising prediction of the ssDNA gap model, namely that DSBs are not fundamental to the mechanism-of-action of genotoxic chemotherapies, but rather a

byproduct of the programmed cell death nucleolytic machinery (Figure 2.9A). To address this possibility, we first confirmed that genotoxic therapy induces programmed cell death via apoptosis. We treated BRCA2 deficient PEO1 with an approximate IC50 dose of cisplatin (0.5uM), and we measured apoptosis with Annexin V and cell death with propidium iodide (PI) in a flow cytometry time course experiment. We observed early apoptosis beginning 24h after treatment, with a minority of cells staining Annexin V positive and PI negative (Figure 2.9B and Figure 2.10A). By 120h after cisplatin treatment, we observed approximately fifty percent of cells were in late apoptosis with Annexin V and PI co-staining, as expected for the IC50 dose (Figure 2.10A). As controls, we confirmed that the BRCA2 proficient C4-2 cells displayed reduced PI and Annexin V signal at all time points following cisplatin as expected (Figure 2.10B). Moreover, in response to high dose camptothecin, a topoisomerase inhibitor that is reported to induce DSBs (30), we confirmed that PEO1 cells were hypersensitive as compared to C4- 2 cells, and underwent apoptosis that was suppressed by the pan-caspase inhibitor Z-VAD-FMK (Figure 2.9B, 2.10C-F) (31). In addition, as a control, we confirmed that treatment with Z-VAD-FMK did not alter cell cycle progression (Figure 2.10G). Taken together, these results indicate that BRCA2 deficient cells undergo programmed cell death via apoptosis after genotoxic treatment.

Finally, we tested if we could detect DSBs following cisplatin or camptothecin. Following approximately the IC90 dose of camptothecin or cisplatin, we isolated intact genomic DNA (gDNA) in agarose plugs, which were subsequently analyzed by pulsed field capillary electrophoresis (Figure 2.9C). As expected, we observed extensive DNA

fragmentation by DSBs in PEO1 cells following 48h treatment with 1uM camptothecin, and to a lesser extent with 24h 2.5uM cisplatin, as indicated by the reduced DNA capillary retention time after treatment that corresponds to sub-megabase sized DNA standards (Figure 2.9D). In contrast, when apoptosis was inhibited with Z-VAD-FMK, we were unable to detect DSBs after either agent, with the capillary retention time corresponding to megabase sized gDNA and indistinguishable from the retention time observed in the untreated controls (Figure 2.9D). Moreover, we found that a second pan-caspase inhibitor, Emricasan, similarly eliminated apoptosis by flow cytometry as well as all detectable DSBs after genotoxin treatment (Figure 2.10H). Taken together, these results support a framework where genotoxic agents create ssDNA gaps, which induce programmed cell death signaling via cleaved caspases to activate the DNA nucleolytic machinery, which ultimately creates DSBs.

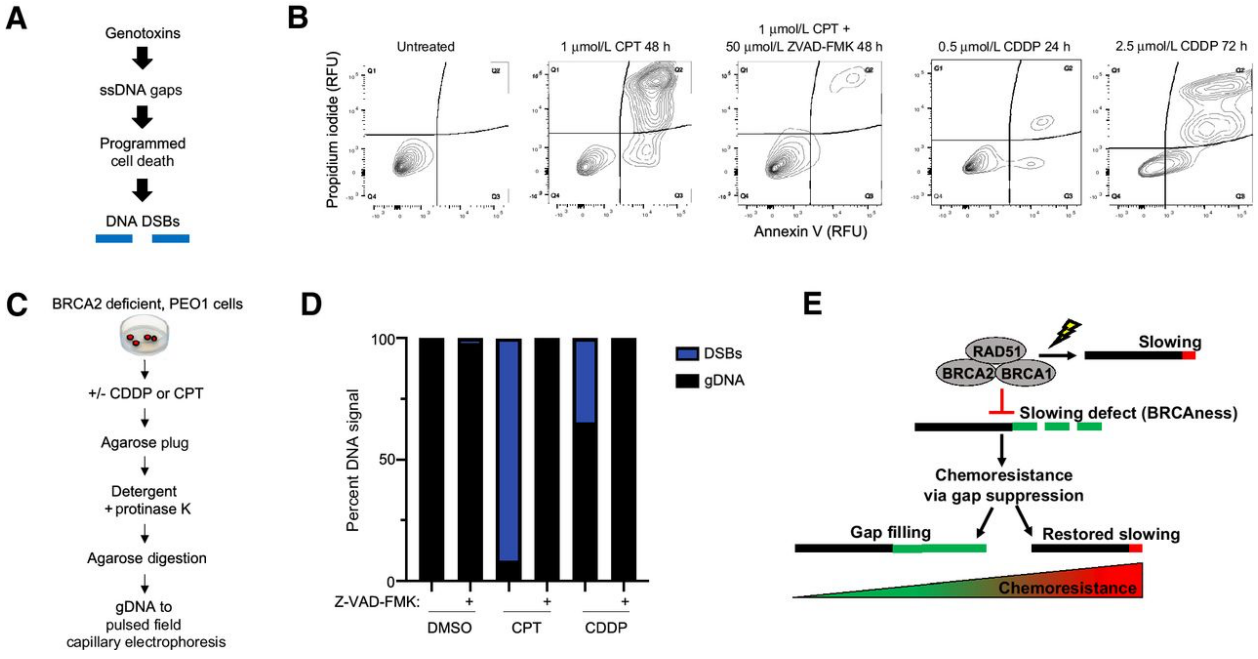

Figure 2.9: DNA DSBs are not detected when apoptosis is inhibited. A, Overview of model. Therapy induces ssDNA gaps that trigger programmed cell death, and the nucleolytic machinery creates DNA DSBs. B, Flow cytometry with

PI and Annexin V shows that apoptosis is eliminated by 50 μmol/L Z-VAD-FMK in BRCA2-deficient PEO1 cells treated with 1 μmol/L camptothecin (CPT) for 48 hours (left). Flow cytometry detects apoptosis in BRCA2-deficient PEO1 cells treated with 0.5 μmol/L cisplatin (CDDP) for 24 hours (see Supplementary Fig. S5A for matched untreated control) or 2.5 μmol/L cisplatin for 72 hours (see Supplementary Fig. S5F for matched untreated control; right). C, Overview of isolation procedure that maintains high molecular weight (megabase scale) gDNA for PFCE. D, PFCE of PEO1 gDNA reveals 50 μmol/L Z-VAD-FMK eliminates all detectable DNA DSBs for both 1 μmol/L camptothecin 48-hour treatment and 2.5 μmol/L cisplatin 24-hour treatment. E, Model of BRCAness and chemoresponse. During stress, BRCA-deficient cells fail to effectively restrain replication, leading to ssDNA gaps that determine chemosensitivity: BRCAness. These cells acquire chemoresistance by eliminating the ssDNA gaps, either by gap filling or by restoring fork slowing.

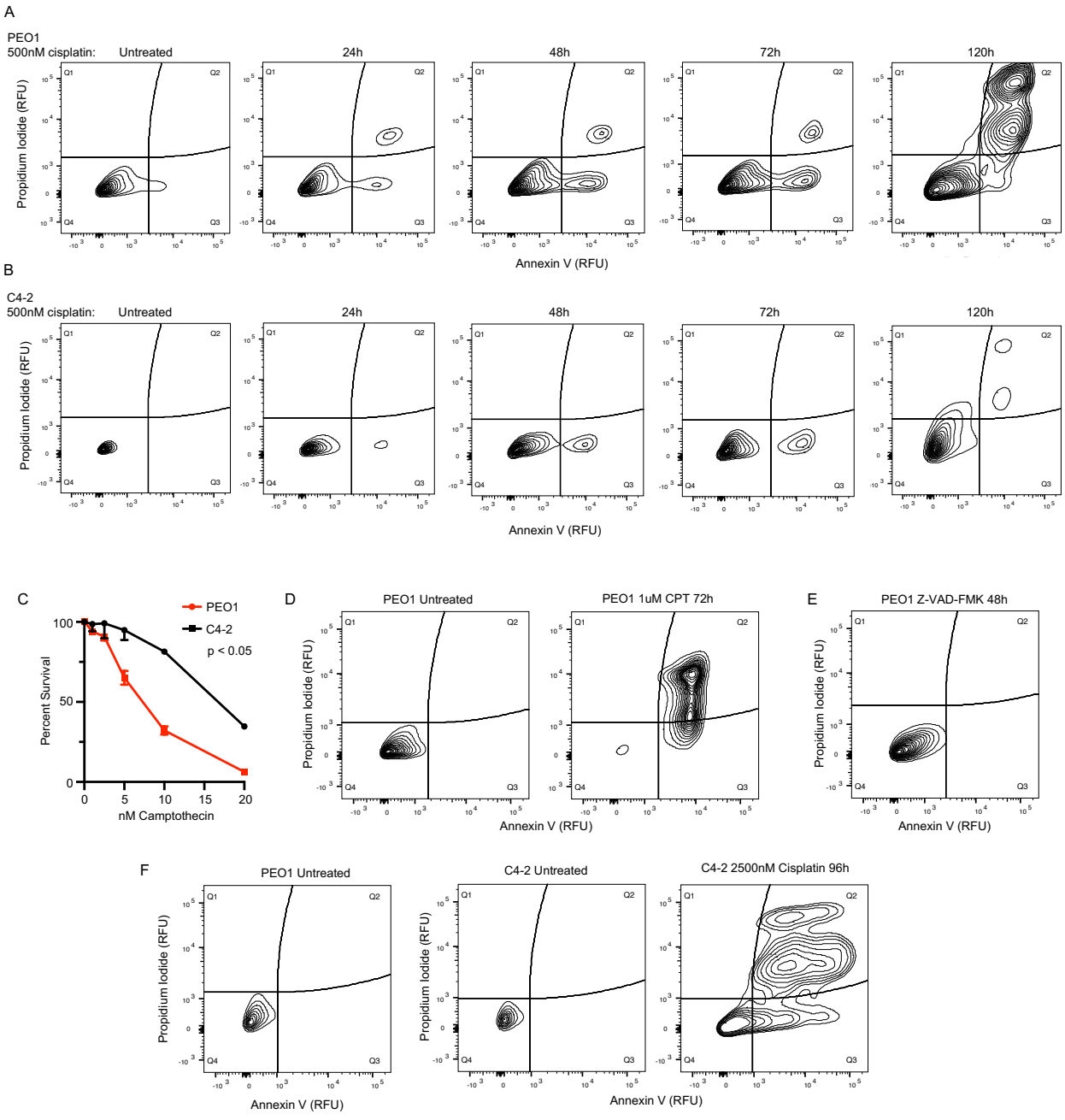

continued

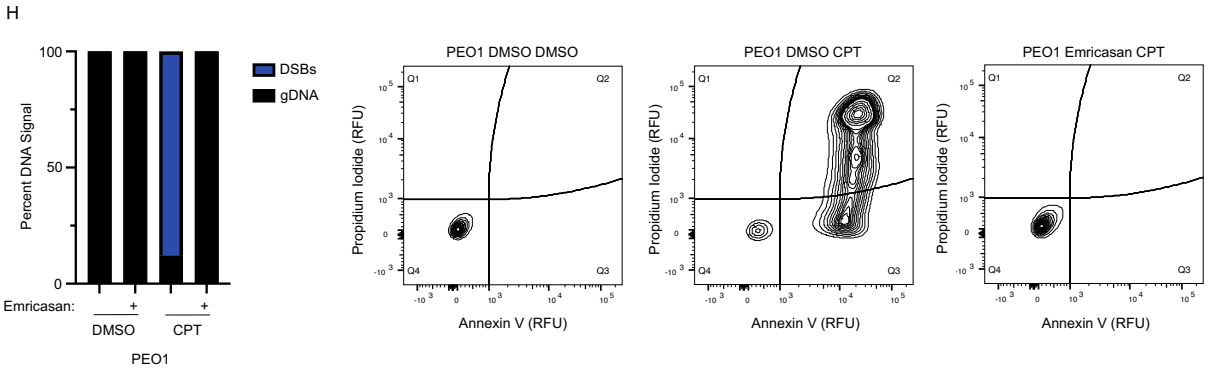

Figure 2.10*:* Apoptosis and Z-VAD-FMK Controls. A) Flow cytometry time course with propidium iodide and annexin V shows that apoptosis is detected at 24h in BRCA2 deficient PEO1 cells treated with 500nM cisplatin, and B) apoptosis is reduced in BRCA2 proficient C4-2. C) Cell survival assay confirms BRCA2 deficient PEO1 cells are hypersensitive to camptothecin compared to BRCA2 proficient C4-2 cells. D) Flow cytometry with propidium iodide and annexin V shows that 1uM CPT for 72h induces apoptosis in PEO1, E) that 50uM Z-VAD-FMK for 48h does not induce apoptosis or cell death in PEO1, F) that 2.5uM cisplatin for 72h induces apoptosis in BRCA2 proficient C4-2 cells; PEO1 untreated control at left matched to Figure 2.9B. G) Flow cytometry with propidium iodide and annexin V shows that the apoptotic inhibitor Z-VAD-FMK does not alter cell cycle progression when administered either alone (top) or with genotoxic agents (bottom). H) PFCE of PEO1 genomic DNA reveals 50uM Emricasan eliminates all detectable DNA DSBs for 1uM CPT 48h (left), and also eliminates all detectable apoptosis as measured by flow cytometry with propidium iodide and annexin V (right).

Discussion

Although ssDNA gaps are a common indicator of genotoxicity and result from loss of the BRCA- RAD51 pathway, they have been overlooked as the determinant of toxicity in favor of defects in HR and FP (6, 12, 28, 30, 32-38). However, there are several genetic systems in which the DSB model does not appear to accurately predict therapy response, and therefore presents an opportunity to revise the underlying framework. Indeed, in light of our findings in different genetic backgrounds, including both BRCA1 and BRCA2 deficient cancers (Figure 2.11), we propose that replication gaps underlie the mechanism-of-action of genotoxic chemotherapies, and it is the failure to suppress gaps, and not defects in HR or FP, that underlies the hypersensitivity of BRCA-deficient cancer to treatment. In support of this concept, when gaps persist, we demonstrate that

HR or FP proficient cells can nevertheless be hypersensitive to genotoxins. Moreover, when gaps are suppressed by loss of CHD4, FEN1, EZH2, or ZFHX3, BRCA2 mutant cells are resistant to genotoxins without restoring HR (21, 23, 24). Similarly, without HR, FP is proposed to mediate cisplatin resistance (18), however we find restored FP in BRCA2 deficient cells achieved by MRE11 inhibition or SMARCAL1 depletion does not enhance cisplatin resistance. We also find that other fork protection factors fail to accurately predict therapy response in the TCGA.

Cell line	HR	FP	GS	Cisplatin Response
BRCA1/2 proficient	+	+	+	Resistant
BRCA2 and CHD4 deficient	-	+	+	Resistant
BRCA2 S3291A mutant	+	-	+	Resistant
BRCA1/2 deficient	-	-	-	Hypersensitive
RAD51 T131P mutant	+	-	-	Hypersensitive
RAD51 T131P mutant and RADX deficient	+	+	-	Hypersensitive
BRCA2 deficient and MRE11 inhibited	-	+	-	Hypersensitive
BRCA2 and SMARCAL1 deficient	-	+	-	Hypersensitive

Figure 2.11: Prediction Table of BRCAness and Chemoresponse. Prediction table demonstrates that the ssDNA gap model accurately predicts chemoresponse. HR is homologous recombination, FP is fork protection, GS is gap suppression, CDDP is cisplatin.

In addition, the emerging evidence indicates that gaps are distinct lesions arising from replication defects, are suppressed by the BRCA-RAD51 pathway, and are located behind the fork at sites distinct from stalled or broken replication forks (28, 37, 39-42). When replication fails to be fully restrained due to loss of the BRCA-RAD51 pathway, we predict that replication gaps derive from replication dysfunction rather than overactive nuclease activity (28, 43). While nucleases could extend nicks or gaps, we found S1 nuclease digestion was unaffected by MRE11 inhibition or depletion of the fork remodeler SMARCAL1, which generates the replication fork structure degraded by MRE11 in BRCA2 deficient cells (27, 28, 44). Thus, gaps likely form in newly replicated

DNA prior to remodeling or degradation of replication forks. We find that gaps are suppressed by at least two mechanisms: gap filling when replication proceeds during exposure to genotoxins, or by restored fork restraint as achieved by BRCA reversion mutation that provides a more robust gap suppression and in turn greater chemoresistance (Figure 2.9E).

Importantly, our findings do not exclude the possibility that ssDNA gaps are in fact converted, albeit at undetectable levels, into DSBs that drive hypersensitivity. However, it is unclear how low levels of DSBs would lead to hypersensitivity, especially considering that BRCA-deficient cells employ backup DSB repair mechanisms, such as end joining pathways. Although the resulting genomic instability introduced by end joining pathways could conceivably trigger hypersensitivity in BRCA cancer, this model does not appear to fit the observed data. Specifically, the FP deficient VC-8 cells with the BRCA2 S3291A mutant display substantial genomic instability, yet simultaneously display cisplatin resistance that is indistinguishable from the WT BRCA2 control (6) (Figure 2.6H, I). Similarly, if ssDNA gaps are ultimately converted into DSBs, then cells proficient for HR would be expected to successfully repair these DSBs and therefore be resistant; however, the Fanconi Anemia RAD51 T131P cells are HR proficient, yet are nevertheless hypersensitive to chemotherapy (12) even when FP is restored (Figure 2.7D, E, 2.8). Indeed, these hypersensitive T131P cells also conflict more generally with models where DSBs are proposed to be the sensitizing lesion, even if the DSBs are assumed to be generated at levels that are undetectable by PFCE/PFGE; why would DSBs cause hypersensitivity in cells that efficiently repair DSBs with HR? In addition,

hypersensitivity with proficient HR has also been observed in other genetic systems (45), suggesting this is not an aberrant observation, and further reduces confidence in DSB models of BRCAness.

Instead, as we report here and as previously shown (46, 47) genotoxin-induced DSBs appear to be created by the programmed cell death process rather than by the genotoxins themselves. Indeed, the observed DSBs from cisplatin and other genotoxic agents result in initial DNA fragments approximately 500-100kb in size (48), which match the early DNA fragments generated by the ordered nucleolytic degradation process carried out by the programmed cell death machinery (49). Accordingly, we also considered that programmed cell death could be the source of the DSBs that cause hypersensitivity; however, we found this model also did not appear to agree with experiment for reasons identical to those described above. In particular, cell death induced DSBs would not be expected to confer hypersensitivity in the HR proficient T131P cells because the DSBs would be effectively resolved by HR repair. Similarly, we also considered that BRCA deficient cells could instead be uniquely “primed” for programmed cell death, leading to increased cell death nuclease activity that creates higher levels of DSBs to overwhelm even intact HR machinery. However, this model is inconsistent with reports that disruption of programmed cell death nucleases eliminates observable DSBs, but does not eliminate programmed cell death or hypersensitivity (50). This observation also indicates that ssDNA gaps likely can induce cell death by a variety of different mechanisms within the programmed cell death repertoire. Therefore, we propose DSBs are generated either as an unrelated byproduct

or as a minority lesion that does not substantially contribute to hypersensitivity, whereas ssDNA gap induced cell killing is the basis for the toxicity of genotoxic agents and BRCAness.

Lastly, we also propose that it will be critical to design experiments to further test both models. Specifically, it will be important to determine if there are latent and unappreciated DSB repair defects in HR proficient cells that are hypersensitive to genotoxins. Likewise, it will be important to determine if persistent ssDNA gaps that occur during active replication under genotoxins can be identified in resistant cells, or if such gaps are found to be absent in hypersensitive cells. Furthermore, it will be important to assess if the cellular introduction of ssDNA or DSB substrates differentially induce programmed cell death as previously described (51, 52); exploring this concept further by gene editing techniques will overcome the limitations of cell transfection and help elucidate the link between ssDNA gaps, DSBs, and genomic instability. It will also be critical to identify gap filling mechanisms that can be targeted to restore hypersensitivity; one possible target is translesion synthesis (TLS). Indeed, CHD4 depletion elevates TLS that suppresses replication gaps (21, 39, 53). Not surprisingly, TLS confers chemotherapy resistance, is a cancer adaptation, and is actively being targeted for cancer therapy (53, 54). Moreover, we find that replication gaps due to BRCA deficiency is the basis for synthetic lethality to PARP inhibitors (55). Understanding how gap suppression functions align with other BRCA roles in genome preservation, cell viability, and tumor suppression will also be critical future questions.

In summary, this study supports a new model that predicts cancer cells with the BRCAness phenotype will be effectively treated by therapies that exacerbate replication gaps. Similarly, preventing gap suppression pathways will improve the effectiveness of therapy as well potentially re- sensitize chemoresistant disease to therapy. Based on our findings, we also propose that ssDNA gaps could serve as biomarkers for BRCAness, and that gap induction is fundamental to the mechanism-of-action of chemotherapies that dysregulate replication.

Materials and Methods

Cell Culture

PEO1, C4-2, VC-8, and MDA-MB-436 cell lines were cultured in DMEM + 10% FBS + 1% P/S. HCC1937 Deficient and HCC1937 + WT BRCA1 were cultured in RPMI1640 + L-Glutamine + 10% FBS + 1% P/S. The Fanconi Anemia RAD51 T131P cells were cultured in DMEM + 15% FBS + Glutamax supplemented with non-essential amino acids. All cells were confirmed mycoplasma free with the MycoALERT kit according to the manufacturer's instructions (Lonza), with the most recent test in September 2020. PEO1 and C4-2 cells were obtained from the Toshi Taniguchi Lab in September of 2014; VC-8 cells were obtained from the Maria Jasin Lab in September of 2014; HCC1937 cells were obtained from the Lee Zhou Lab in October of 2017; and the RAD51 T131P cells were obtained from the Agata Smogorzewska Lab in January of 2019. The MDA-MB-436 were obtained from ATCC and validated by STR profiling. Cells were validated by western blot and/or Cell Titer Glo toxicity assays as described in

the manuscript. Cells were briefly expanded to frozen stocks and used in experiments within ten passages.

DNA Fiber Assays

DNA fiber assays were performed as previously described. Briefly, cells were plated at 10^6 cells per 10cm dish and allowed to adhere for 36h. Subsequently, DNA was labeled for 30 minutes with 50uM IdU and washed with PBS, and treated with 50uM CldU and replication stress depending on the assay. For fork restraint assays, cells were exposed to 50uM CldU with 0.5mM HU for 2h. For fork restraint with continued stress, cells were exposed to 50uM CldU with 0.5mM HU for 2h, followed by 4mM HU for 2-3h. For fork degradation assays, cells were labeled with 50uM CldU alone, followed by 4mM HU for 3-5h. After labeling, cells were collected with trypsin, washed with PBS, and resuspended in PBS at 250,000 cells/ml. 2ul of cell solution was placed on a positively charged slide, followed by lysis for 8 minutes with 12.5ul of spreading buffer (0.5% SDS, 200mM Tris-HCl, pH 7.4, 50mM EDTA). Slides were tilted to a 45 degree angle to allow fibers to spread, allowed to dry for 20 minutes, fixed in 3:1 Methanol:Acetic Acid for 3 minutes, rehydrated in PBS for 5 minutes, denatured with 2.5mM HCl for 30 minutes, blocked with PBS + 0.1% TritonX-100 + 3% BSA for 1h, and treated with primary (2.5h, 1:100) and secondary antibodies (1h, 1:200) in PBS + 0.1% TritonX-100 + 3% BSA. Slides were washed with PBS and mounted with ProLong Gold antifade. Track lengths were measured in Fiji (16). The antibody used to detect IdU was anti-BrdU (Becton Dickinson 347580, detects both BrdU and IdU); the antibody used to detect CldU was anti-BrdU (Abcam ab6326, detects both BrdU and CldU). The secondary antibodies

used were Alexa 488 anti-mouse (detects the primary IdU antibody) and Alexa 594 anti-rat (detects the primary CldU antibody).

Non-Denaturing ssDNA Fiber Assay

The nondenaturing fiber assay to detect ssDNA was performed using the DNA Fiber Assay protocol above with the following modifications: first, all acid steps were removed (both acetic acid from the fixation step, and the HCl denaturing step), and EDTA was removed from the lysis buffer (EDTA impairs Click Chemistry). In addition, IdU was replaced with EdU and detected by ClickIT EdU Alexa 488 Imaging Kit (Thermo Scientific) to label analog in non-denatured DNA per the manufacturer's instructions. After Click Chemistry, ssDNA was detected by incubating DNA with the primary anti-BrdU antibody (Abcam ab6326, detects both BrdU and CldU) and the secondary antibody Alexa 594 anti-rat as described above. Images were analyzed in Fiju. We classified ssDNA-positive forks based on their line graph; specifically, if ssDNA signal was found adjacent to the EdU labeled regions, the fork was classified as ssDNA positive. In contrast, if there were no regions of ssDNA signal adjacent to the EdU, the fork was classified as ssDNA negative.

S1 Nuclease Fiber Assay

As described previously, cells were exposed to 50uM IdU to label replication forks, followed by 50uM CldU with 0.5mM HU for 2h. Subsequently, cells were permeabilized with CSK buffer (100 mM NaCl, 10 mM MOPS, 3 mM MgCl2 pH 7.2, 300 mM sucrose, 0.5% Triton X-100) at room temperature for 8 minutes, followed by S1 nuclease

(20U/ml) in S1 buffer (30 mM Sodium Acetate pH 4.6, 10 mM Zinc Acetate, 5% Glycerol, 50 mM NaCl) for 30 minutes at 37C. Finally, cells were collected by scraping, pelleted, resuspended in 100-500ul PBS; 2ul of cell suspension was spotted on a positively charged slide and lysed and processed as described in the DNA fiber assay section above.

PDX Methods

PNX0204 was derived at Fox Chase Cancer Center under IRB and IACUC approved protocols. PDX tumors were grown in NOD.Cg-Prkdc^{scid} Il2rg^{tm1Wjl}/SzJ (NSG) mice. Cisplatin resistant PDX tumors were obtained from mice after tumors progressed on serial treatments of 6 mg/kg cisplatin. The tumors were harvested at approximately 500 mm^3 and dissociated in 0.2% collagenase, 0.33 mg/ml dispase solution for 3h at 37°C. The dissociated cells were maintained at 37°C in RPMI1640 + 10% FBS and used for DNA fiber assays within 24h of tumor extraction. DNA fiber and S1 nuclease fiber assays were performed as described above.

Supplementary Materials and Methods

Drugs

All drugs were prepared according to the manufacturer's instructions. Cisplatin (Sigma) was prepared as a 1mM solution in saline and added to complete media. HU was prepared fresh from powder in complete media prior to experiments. The MRE11 inhibitor Mirin (Sigma) was prepared as a 50mM solution in DMSO and used at 50uM in

complete media for DNA fiber analysis and was added during the indicated step per the figure diagrams (1). For toxicity assays, mirin was added at 10uM (to adjust to the 96 well format) with cisplatin or saline for 18h. EZH2 was inhibited with 5uM GSK126 (Selleck) solubilized in DMSO and was added in complete medium during the CldU + HU step in fiber analysis (2). 5-chloro-2′-deoxyuridine (CldU), 5-Iodo-2′-deoxyuridine (IdU), and 5-Ethnyl-2'-deoxyuridine (EdU) were obtained from Sigma and solutions were prepared per the manufacturer's instructions in water and DMSO and DMSO, respectively, and added in complete medium for fiber experiments. The pan-caspase inhibitors Z-VAD-FMK (Selleck) and Emricasan (Selleck) were prepared in DMSO, and cells were pretreated with 50uM Z-VAD-FMK or Emricasan for 2h in complete media prior to treatment with genotoxins and subsequently maintained at a 50uM concentration throughout the experiment. Camptothecin (Sigma) was solubilized in DMSO and added to complete media for toxicity experiments.

shRNA

HEK293T cells were used to package lentiviral particles with the pLKO.1 shRNA system as previously described (3). Briefly, HEK293 cells were transfected with 1:1:2 µg of packaging plasmids versus shRNA hairpins on the pLKO.1 vector using Effectene transfection reagent (Qiagen) 48 h prior to harvesting supernatants. Supernatants were filtered and added to recipient cell lines with 1 µg/mL polybrene. Cells infected with shRNA vectors were selected with puromycin. For shRNA-mediated silencing, the following hairpins from The RNAi Consortium were obtained from GE Dharmacon: CHD4-61 (B), TRCN0000021361: 5'-GCTGACACAGTTATTATCTAT-3'

CHD4-62 (A), TRCN0000021362: 5’-GCTGACACAGTTATTATCTAT-3’

ZFHX3-58, TRCN0000013558: 5′-GCCAGGAAGAATTATGAGAAT-3′

FEN1-32 (B), TRCN0000049732: 5’-GATGCCTCTATGAGCATTTAT-3’

SMARCAL1-69, TRCN0000083569: 5’-GCGGAACTCATTGCAGTGTTT-3’

RADX-85 (A), TRCN0000128185: 5’-CTGAAAGTATTCCACGGAAAT-3’

RADX-208 (B), TRCN0000147208: 5’-CCAAAGCTAAATCACCGATTT-3’

CellTiter-Glo 2.0 Toxicity Assays

Cells were plated at 500 cells per well in the center wells of a 96 well plate in 200ul volume and allowed to adhere for 36h. Subsequently, drugs were added in a 100ul volume and the cells were incubated for 10 days; mirin assays were incubated for 18h and subsequently changed to fresh media for the remainder of the assay. CellTiter-Glo 2.0 (Promega) was used to quantify cell number by ATP. To prevent evaporation, all blank wells in the 96 well plate were filled with media, and each plate was placed in a humid chamber with PBS containing antibiotic and antimycotic (Thermo Scientific).

Dynamic Molecular Combing of Cisplatin-DNA Fibers

We employed Dynamic Molecular Combing as previously described (4) to improve the quality of DNA fibers from cells treated with cisplatin. Briefly, 106 cells were plated into 10cm dishes and allowed to adhere for 36h. Cells were then treated with IdU for 30 minutes, washed with PBS, and treated with CldU + 1000nM cisplatin for 2h; untreated controls were treated with CldU without cisplatin for 2h. Subsequently, cells were trypsinized, resuspended in PBS, and prepared as agarose plugs with 100,000 cells per

plug. Plugs were allowed to solidify at 4□C for 30 minutes, and were subsequently digested in ESP buffer (EDTA, Sarcosyl, and Protinase K) for 48h at 50□C. Plugs were subsequently washed to remove debris, melted at 68□C for 20-30 minutes, and then digested in combing reservoirs with beta-agarase overnight at 42□C. The next day, gDNA solutions were combed in 0.5M MES (pH 5.7) onto silanized coverslips using the coverslip combing apparatus from Genomic Vision. gDNA was baked onto coverslips at 60□C overnight, and analogs were detected as described in the DNA Fiber Analysis section above (starting after, but not including, the Methanol/Acetic Acid fixation step). Silanized coverslips were prepared as previously described (4); briefly, coverslips were cleaned extensively with sonication, dried, and surfaces were activated by Argon plasma cleaning using a Harrick Plasma cleaner. Subsequently, coverslips were exposed to air to prepare surface hydroxyl groups, dried at 60°C to remove excess water vapor, and silanized with Octenyltrichlorosilane by chemical vapor deposition overnight using a vacuum desiccator. Coverslips were subsequently washed and sonicated with chloroform to remove excess silane. All silanization steps were performed in an inert and dry environment (nitrogen glove bag) to prevent spontaneous silane polymerization.

EdU Global Cellular Replication Assay

100,000 cells were plated onto poly-l-lysine coated coverslips and allowed to adhere for 36h. Cells were subsequently treated with EdU with or without drug as indicated, fixed, and processed for Click-IT EdU detection according to the manufacturer's instructions (Thermo Scientific). Coverslips were mounted in Vectashield with DAPI, and ten fields

were imaged at 20x in the center of the coverslip. EdU intensity per cell was quantified with Cell Profiler from the Broad Institute (5).

Cell Fractionation

To isolate cytoplasmic, nuclear, and chromatin fractions for western blot or mass spectrometry, cells were lysed with the NE-PER kit according to the manufacturer's instructions (Thermo Scientific). To isolate chromatin fractions, the insoluble pellet that remains from NE-PER lysis was resuspended in 60ul of 2x loading buffer with DTT, heated at 70C for 10 minutes, and sonicated in a BioRuptor (Diagenode) for 20 minutes on high, with a cycle of 30 seconds on and 30 seconds off.

Western Blot

All steps were performed according to the manufacturer's instructions (Thermo Scientific). The protein concentration of different cellular fractions was determined by BCA Assay (Thermo Scientific). Samples were reduced with DTT in LDS loading buffer, and heated at 70C for 10 minutes. 40ug total protein was fully resolved on either a Tris-Acetate gel (for large proteins) or a Bis-Tris gel (for small proteins), and transferred to a nitrocellulose membrane. The nitrocellulose membrane was processed for near-infrared quantitative westerns according to the manufacturer's protocol (LiCor). The membrane was allowed to dry for 20 minutes (or overnight), total protein was stained with the REVERT stain as a total protein loading control, followed by blocking with Odyssey blocking buffer, treated with primary antibody overnight, followed by near-infrared secondary antibody (800CW) at 1:5000 for 1h. The membrane was allowed to dry prior

to imaging on the LiCor Odyssey Imager. Primary antibodies used include anti-BRCA2 (Abcam ab123491, 1:1000); anti-CHD4 (Abcam ab54603 1:1000); anti-CHD4 (Abcam ab70469, for immunoprecipitation); anti-SMARCAL1 (Abam ab37003, 1:1000); anti-ZFHX3 (Lifespan Biosciences LS-C179898-100); anti-PCNA (Abcam ab29); anti-B-actin (Sigma A5441, 1:15,000).

Proteomics

For SILAC, PEO1 were dual labeled in SILAC media with dialyzed FBS (Thermo Scientific) with heavy lysine (K+8) and heavy arginine (R+10) from Cambridge Isotope Labs. PEO1 and C4-2 (unlabeled SILAC media) were treated with cisplatin, collected with trypsin, counted, mixed at a 1:1 ratio, and fractionated together in the same Eppendorf tube with the NE-PER kit as described. Cellular fractions were fully resolved on SDS-PAGE gels, fixed with Imperial Protein Coomassie Stain (Thermo Scientific), washed in water overnight to remove excess stain, and cut into 13 molecular weight regions corresponding to the protein marker standard. Each region was reduced with DTT, alkylated with iodoacetamide, and digested with Trypsin Gold for Mass Spectrometry with ProteaseMAX according to the manufacturer's instructions (Promega). Peptides were dried in a speedvac, resuspended in 6 ul buffer A (0.1% formic acid), and 2 ul tryptic digests were analyzed on the Thermo Q-Exactive mass spectrometer coupled to an EASY-nLC Ultra system (Thermo Fisher). Peptides were separated on reversed phase columns (12 cm x 100 μm I.D), packed with Halo C18 (2.7 um particle size, 90 nm pore size, Michrom Bioresources) at a flow rate of 300 nl/min with a gradient of 0 to 40% acetonitrile (0.1% FA) over 55 min. Peptides were injected

into the mass spectrometer via a nanospray ionization source at a spray voltage of 2.2 kV. The mass spectrometer was operated in a data-dependent fashion using a top-10 mode (6).

Processing of Proteomics Data

Raw proteomics data were analyzed with MaxQuant software (7). We required a false discovery rate (FDR) of 0.01 for proteins and peptides and a minimum peptide length of 7 amino acids. MS/MS spectra were searched against the human proteome from UniProt. For the Andromeda search, we selected trypsin allowing for cleavage N-terminal to proline as the enzyme specificity. We selected cysteine carbamidomethylation as a fixed modification, and protein N-terminal acetylation and methionine oxidation were selected as variable modifications. Two missed tryptic cleavages were allowed. Initial mass deviation of precursor ion was up to 7 ppm, mass deviation for fragment ions was 0.5 Dalton. Protein identification required one unique peptide to the protein group. Known contaminants were removed from the analysis. To identify statistical significance, isotopic ratios of identified proteins from three biological replicates were analyzed using the limma statistical package (8). The isotopic ratio obtained from MaxQuant was subsequently converted to log2 scale and plotted against the -log10(p-value) for each gene in GraphPad Prism.

TCGA Database Analysis

The TCGA database was used to identify ovarian cancer patients with germline mutations in BRCA2, and subsequently tested for predictive power of mRNA expression

of genes of interest on patient progression free survival. To obtain patient germline sequencing data, we applied for access to protected TCGA patient data through NIH. The germline BAM sequencing data for each patient at the BRCA2 locus was downloaded. The BAM Slicing tool option and the GDC API were used to automate the process. Sliced BAM files were sorted and indexed using SAMTOOLS (9), and mutations were identified using the Genome Analysis Tool Kit (GATK, Broad Institute) (10). We followed the GATK best practices for germline mutation calling until the last step of the protocol, where we used hard filtering instead of variant quality score recalibration (VQSR) because sliced BAM files at a single locus are not compatible with VQSR. Briefly, we called germline variants using the HaplotypeCaller tool in GVCF mode, consolidated the GVCF files using the GenomicsDBImport Tool, and called mutations using the GenotypeGVCFs tool. The data were hard filtered to isolate BRCA2 germline mutations, and we classified mutations using the Variant Effect Predictor (VEP) from Ensembl (11). Finally, mutations were selected that are predicted to disable BRCA2, including premature stop codons, frameshift mutations, and deletions. A case list of patient barcodes was compiled harboring at least one of these BRCA2 disabling mutations, and cBioPortal and the TCGA-CDR (12-14) were used to obtain the progression free survival data and mRNA expression data (from the U133 Microarray, which was the most complete dataset for all genes except for KMT2B, for which we used the RNAseq data) for our genes of interest in this set of patients. To eliminate bias and subjectivity, patients with mRNA expression of the target gene over the median were classified as high expression; patients below were classified as low expression. The survival curves for the low and high expression groups were plotted with the

lifelines package for Python, and significance was determined using the Cox regression (15).

Flow Cytometry with Annexin V and Propidium Iodide

Cells were assayed for Annexin V and Propidium Iodide signal following the manufacturer's instructions (Abcam). Briefly, PEO1 were plated at 100,000 cells per 10 cm plate and allowed to adhere for 36h. Subsequently, the media was aspirated and replaced with 40ml of complete medium containing 500nM cisplatin in order to match the molar ratio of drug to cells found in the 96 well Cell Titer Glo assay (16). At 0h, 24, 48, 72, and 120h, cells were trypsinized (including floating cells in the media), washed, stained with Annexin V and PI, and analyzed on a BD LSR II flow cytometer in the FITC and PI channels. Cells treated with 1uM camptothecin for 48h were processed identically. For inhibition of apoptosis with Z-VAD-FMK, cells were pretreated for 2h with 50uM Z-VAD-FMK, and subsequently treated with cisplatin or camptothecin in media containing 50uM Z-VAD-FMK. Untreated controls were treated with DMSO as a vehicle control for Z-VAD-FMK and camptothecin. Quadrants for Annexin V signal, PI signal, and Annexin V and PI co-signal were selected based on the staining of the untreated control. For cell cycle controls, cells were collected after treatment, fixed on ice with 70% ethanol with vortexing, resuspended in PBS with RNAse and propidium iodide, and on a BD LSR II flow cytometer in the PI channel; single cells were selected to eliminate clumped cells from the analysis.

DNA Pulsed Field Capillary Electrophoresis

PEO1 were assayed for DSBs by pulsed field capillary electrophoresis with the Femto Pulse (Agilent). Briefly, 100,000 cells were plated per 10 cm plate and allowed to adhere for 36h. Subsequently, the media was aspirated and replaced with 40ml of complete medium containing 2.5uM cisplatin in order to match the molar ratio of drug to cells found in the 96 well Cell Titer Glo assay (16), or 1uM camptothecin; cells treated with apoptotic inhibitor were pretreated for 2h with 50uM Z-VAD-FMK and maintained for the duration of the experiment, and untreated controls received DMSO as a vehicle control. At 24h (for cisplatin) or 48h (for camptothecin), cells were trypsinized (including floating cells in the media), pelleted, and washed, and high molecular weight gDNA was isolated with the FiberPrep Genomic DNA Extraction Kit (Genomic Vision) according to the manufacturer's instructions; the final digestion step was supplemented with an additional 5ul of beta-agarase to ensure full digestion of the agarose plug (New England Biolabs). gDNA was analyzed on the Femto Pulse in the 3.5h mode for gDNA and large fragments per the manufacturer's instructions (Agilent). The retention time of gDNA and DSBs was experimentally determined, with intact gDNA observed as signal above 8,000 seconds of capillary retention time, and DNA DSBs and fragmentation observed in the 3000 second to 8000 second window of capillary retention time; the percent of signal from gDNA and DSBs were plotted in Graph Pad Prism.

CHAPTER III: DISCUSSION

Expanded Discussion

Summary and Conclusions: This dissertation proposes a new ssDNA theory of BRCAness and genotoxic agents and argues for a reconsideration and possible overturn the previous double strand break framework. The body of work demonstrates the ssDNA framework has superior predictive power with less complexity than the dogma for all genetic systems tested, including known, new, and edge cases, and establishes the theory as a legitimate competing framework. Moreover, the ssDNA theory accurately predicts that the double strand breaks observed after genotoxic therapy are in fact created by the apoptotic machinery and not by the drugs themselves, undermining confidence in the double strand break dogma.

Complexity	Inconsistency
Double strand breaks are below detection	FA T131P RADX Abundance of ssDNA Backup repair, e.g. MMEJ
Backup repair leads to hypersensitivity via instability	Instability does not predict hypersensitivity BRCA S3291A resistant, unstable Latent levels of DSBs cause massive instability?
Apoptotic DSBs may drive hypersensitivity	Inhibition of apoptotic DSBs does not eliminate death or reduce toxicity; committed to death FA T131P RADX

Table 3.1*: An example of added dogma complexities that are difficult to reconcile with experiment.*

We propose these results place the ssDNA theory as the leading framework for BRCAness and genotoxic agents, and that confidence in the double strand break dogma is accordingly reduced to lower levels. Indeed, we considered a number of

complexities that could be added as an attempt to rescue the dogma, but found these inconsistent with experiment as they are currently understood (*Table 1*). However, we propose it is important that these two frameworks directly compete in order to improve experimental power, and we highlight here several important future experiments and the limitations of current technical approaches that should be improved. In addition, this section will highlight the broader implications of the ssDNA theory that were not discussed in the publication, including for DNA metabolism disorders, and will cover important future technologies, both for patient diagnostics as well as for improved mechanistic understanding of the ssDNA defect.

Possibilities to Salvage the Dogma: Time Course of DNA Double Strand Breaks

Future experiments should analyze the creation of DNA double strand breaks and ssDNA over time, with the goal of determining the earliest possible time point of their visibility, their approximate abundance, their predictive power for sensitivity, and if they are apoptotic. Indeed, it is possible that low levels of double strand breaks could be created at early time points, even minutes after treatment, that commit the cells to undergoing apoptosis; however, we propose such a result would represent a contributing role for double strand breaks within an ssDNA framework due to the abundance, toxicity, and predictive power of ssDNA. Importantly, if such breaks are detected, their repair may not be sufficient to rescue the cell after a signal to die has been sent; similar concepts apply for ssDNA and should be elucidated to ensure the correct time point for critical mechanistic and signaling events can be analyzed[1]. In

addition, we note here that apoptotic inhibitors should be used to control for a role in apoptosis in generating ssDNA; we did not complete this control in our publication because apoptosis is not reported to cause deficient replication fork arrest to the best of our knowledge.

ssDNA in Genome Stability and Cancer Initiation

Given the role of ssDNA as a critical BRCA gene function, phenotypes previously assigned to double strand breaks or fork protection will need to be reevaluated for a basis in ssDNA, including genomic instability and cancer initiation. Indeed, in normal, precancerous breast tissue[2], recent reports indicate patients with a germline mutation in BRCA2 (haploinsufficiency) display a phenotype consistent with ssDNA gaps. Specifically, cells from such patients display an impaired replication stress response as measured by increased analog incorporation during stress similar to the assays described in this dissertation, which may indicate the presence of a fork restraint defect that results in ssDNA even in precancerous tissue. Moreover, this checkpoint defect is associated with an increased DNA damage response and increased DNA mobility in comet assays, again as would be expected if ssDNA were present. Given these reports, it is conceivable that ssDNA is present with BRCA haploinsufficiency, and that these ssDNA gaps lead to genomic instability that initiates the cancer via loss of the wild type allele to create the full BRCAness phenotype. Importantly, the BRCA haploinsufficient cells were also observed to display a defective apoptotic response as measured by reduced staining in the TUNEL assay in normal breast tissue; this could reflect a

tolerization to apoptosis via consistent exposure to ssDNA that allows mutations to accumulate and removes yet another barrier to cancer initiation.

These reported observations are consistent with our ssDNA framework of BRCAness and indicate that suppression of ssDNA gaps is an appealing target for cancer prevention. Indeed, because defects in double strand break repair and fork protection have not been reported with BRCA haploinsufficiency to the best of our knowledge, it is reasonable to speculate that ssDNA is the initiating lesion that ultimately leads to the stronger genomic instability observed upon loss of heterozygosity of the wild type BRCA allele and the resulting fork protection defect. Moreover, recent reports indicate that ssDNA replication gaps are formed in BRCA deficient cells even due to normal cellular metabolism[3], further implicating ssDNA as the fundamental lesion that leads to instability and loss of heterozygosity to initiate the cancer.

The Role of ssDNA in Fanconi Anemia and DNA Metabolism Disorders

Similar to cancer initiation, ssDNA could be the fundamental lesion that underlies the defects of Fanconi Anemia given that ssDNA may form in BRCAness cells during basic cellular metabolism. These metabolic ssDNA lesions could explain the hematological failure found in Fanconi Anemia, as the rapidly replicating cells of the bone marrow accumulate ssDNA due to defects in fork restraint from the Fanconi mutations; defects in homologous recombination, possibly at these ssDNA lesions, could also explain such

hematological defects. Similarly, a central role for ssDNA could also be found for the neuronal cell death that is observed in Fanconi Anemia patients.

However, given the extreme phenotype of Fanconi Anemia, it is important to consider that defects in fork protection and DNA double strand break repair play a significant role in both cellular failure as well as cancer initiation. Nevertheless, defective fork restraint leading to ssDNA could exacerbate the requirement for both fork protection and homologous recombination, and may be an important therapeutic target. It will be important to determine if restoring fork restraint, gap filling, or the possible role of homologous recombination at ssDNA lesions, could be deployed as therapeutics for Fanconi Anemia patients. Similar principles for ssDNA should also be evaluated for other DNA metabolism disorders that result in developmental defects and neurodegeneration, such as Cockayne Syndrome[4].

Some thoughts on the nature of the ssDNA lesion

Our theory proposes that ssDNA is the fundamental lesion of BRCAness, but beyond a dependence on DNA replication and conservation among genotoxins, the physical and molecular details are unknown. Several ideas have been already been proposed, including fork traversal, separation of the leading and lagging strand, and gaps emerging in the daughter strand, and all should be examined.

However, a possibility that has not been explored is the concept of "*piled up forks*," which is mechanistically distinct and provides additional rationale for fork restraint. In a preliminary DNA combing experiment analyzed by atomic force microscopy[5], we observed a structure containing a replication fork with two additional replication forks trailing behind: one on each copy. Moreover, the two trailing replication forks appeared to contain long regions of ssDNA in each of the resulting copies. Could these structures be the ssDNA regions we had detected? If so, the mechanism highlights additional importance for fork arrest: if one fork stalls, perhaps the forks behind must also be arrested to prevent the formation of this structure. Could the slowing defect observed in BRCAness cells lead to this fork pile-up that we detect as ssDNA by light microscopy methods? In addition, the possibility highlights what could be a highly aberrant replication process in cancers, and could help to explain the gene duplications, copy number variations, and genomic instability that are characteristic of the disease.

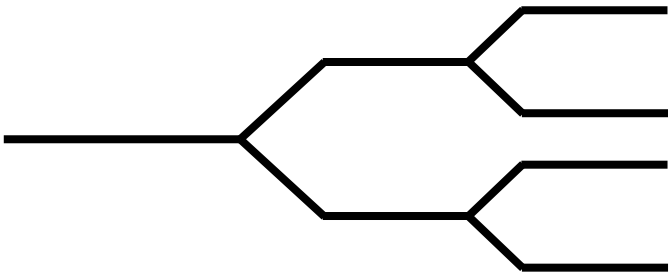

Figure 3.1: Example of "*piled up forks*" observed by atomic force microscopy on combed gDNA. The facility locked down due to COVID during the experiment, so no image could be saved. Could these be the ssDNA structures?

Moreover, with the establishment of dynamic molecular combing in BRCA cells as described in this dissertation, future combing experiments should be conducted to deepen our understanding of replication defects in BRCAness. What is the inter-origin

distance in hypersensitive and resistant BRCA cells? Are new origins and forks fired during stress? Are there defects in initiating and terminating replication forks? These important aspects of replication should be analyzed for a role in hypersensitivity and resistance.

Finally, a role for mitochondrial DNA should be specifically considered and tested using combing and atomic force microscopy technology, especially considering the role of RAD51 in maintaining mtDNA[6]. Indeed, the mtDNA has been demonstrated to efficiently label with the same analogs used in DNA fiber assays, is readily isolatable from gDNA and other cellular components, and can be combed on silanized surfaces, either in linearized or circular form[7]. Are ssDNA regions created in mtDNA as well? Do they accurately predict response? Can the proteome be obtained to find protein mediators? These questions should be addressed given the critical role of the mitochondria in apoptosis[8]. Moreover, the mtDNA could be used as an incredibly sensitive method for double strand break detection after genotoxins: a double strand break will linearize the mitochondrial genome. Such an approach could be used to monitor the number of double strand breaks over time to determine if they are effectively resolved in BRCAness cells, and the method may be more sensitive than pulsed field experiments or DNA combing of gDNA to measure fragmentation.

A Possible Role for Polycomb?

Our systems biology analysis of the BRCA patients in the TCGA implicates the polycomb group genes as critical to hypersensitivity (see *Appendix II*)[9]. Specifically, the top predictive gene in the BRCA2 ovarian cohort is PHC2, a polycomb gene member that does not appear to be well studied in humans. Low PHC2 mRNA predicts poor patient survival consistent with acquired chemoresistance. Most strikingly, a literature search indicates that CHD4 and EZH2 interact with polycomb members[10]; ZFHX3/4 and FEN1 interact with CHD4, and may interact with polycomb as well.

As the polycomb genes represent a large, repressive complex, could removing such a complex from replication sites be creating space for other proteins to bind and resolve ssDNA at the fork? Importantly, more relaxed chromatin appears to be consistent with our observation that depletion of CHD4, EZH2, ZFHX3, and FEN1 appeared to increase replication permissivity in addition to filling gaps. Indeed, this is also consistent with the concept of TLS or repriming being activated to fill gaps. Such a model would also fit with a competitive model of DNA repair choices, where a set of factors must be removed to allow new mediators access to the lesion. Mechanistically, we currently favor this competition model of physical access to the replication fork for proteins such as PHC2, CHD4 and ZFHX3, rather than their roles in gene regulation, for determining hypersensitivity and resistance.

If the polycomb complexes were removed, what factors would take their place to confer resistance? Here, the TCGA implicates LIG4 – with high LIG4 levels predicting one of the worst survival profiles in the dataset. LIG4 is a DNA ligase previously associated

with repairing double strand breaks via NHEJ, but would also be perfectly consistent with translesion synthesis or repriming. However, rather than developing individual hypothesis, we propose an shRNA screen of the top TCGA candidates, after examining larger BRCA patient cohorts, would be more effective in constructing a framework. Indeed, all of the factors on the right side of the graph in *Appendix II* represent potential drug targets to disrupt resistance.

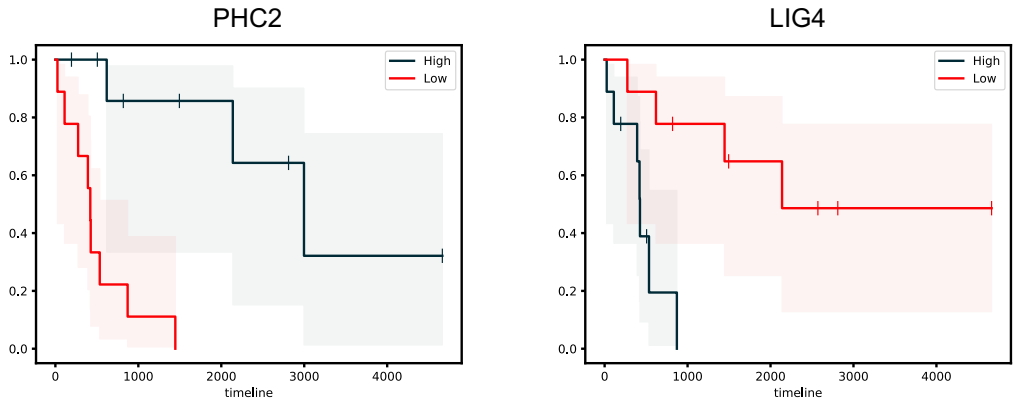

Figure 3.2: Low PHC2 or High LIG4 mRNA predict poor BRCA2 ovarian cancer patient response.

Generalization of the ssDNA Framework Across Genotoxins

With the development of DNA combing, other genotoxins should be explicitly tested to determine if they also produce a slowing defect and ssDNA in BRCAness cells. Although ssDNA is a well-known lesion that is generated after genotoxic therapy, these agents should be specifically tested for ssDNA behind the replication fork that predicts response as we report here. Our report utilized hydroxyurea as a model for genotoxins because hydroxyurea generates high quality fibers that are not covalently damaged; we propose our extrapolation to the broader class of genotoxins was justified based on our observation that the ssDNA framework was accurate for PARPi, which generated

ssDNA identical to hydroxyurea; the observation of the slowing defect with cisplatin; and observation that ssDNA accurately predicted patient response in the TCGA in breast and ovarian cancers, which are treated with a wide range of genotoxic agents, including platinum, PARPi, doxorubicin, ionizing radiation, and taxanes. We propose these agents should be explicitly tested for predictive ssDNA by combing, which improves the quality of even covalently damaged fibers, perhaps because the increased stretching allows the denaturing process to be more effective to visualize the incorporated analogs.

Advanced Technologies to Detect ssDNA and DNA Lesions

We propose it will be important to develop several advanced technologies to detect ssDNA, both for patient diagnostics and for improved mechanistic understanding of BRCAness. More specifically, we propose that the field should embrace technologies that physically assay the gDNA and the structure of the DNA replication fork, rather than relying on indirect methods such as foci and genetics. Physical analysis of the DNA polymer should be preferred to assuming particular fork structures based on genetics and gene depletions, or using protein phosphorylation events as indicators of specific DNA lesions, rather than as general indicators of stress or damage.

Technologies for Patient Diagnostics

For patients, we propose the best possible diagnostic test appears to combine dynamic molecular combing of DNA with atomic force microscopy[5,11,12]. Indeed, dynamic

molecular combing presents several important advantages for diagnostics compared to other DNA fiber analysis methods. First, large numbers of intact gDNA fibers are combed linearly, as opposed to tangled fibers, which improves consistency and reproducibility that will be required for patient diagnostics. Second, this improved fiber distribution from combing also opens up the potential for reliable image analysis from software to greatly improve the speed and reliability of results. Third, dynamic molecular combing is a method that maximizes the integrity of gDNA and the associated DNA structures, including replication forks and ssDNA regions. Importantly, the DNA isolation protocol for DNA combing is identical to that used for pulsed field gel electrophoresis to maintain mega-base sized gDNA. The physical process of combing is extremely gentle because it relies on the meniscus of water to deposit and straighten the intact gDNA, which is estimated to result in forces of less than ten pico-newtons and far is superior to other methods - which require pipetting, nuclease digestion, or chromatography - to preserve the integrity of any gDNA structures that could predict BRCAness and therapy response. Lastly, analysis by atomic force microscopy not only presents picometer resolution - the DNA helix is easily visible - but also does not require analog labeling or nuclease treatments, which makes for a simpler diagnostic test: simply biopsy, lyse, and comb. Samples can be readily stored as plugs for weeks in any physician's office and shipped stably for analysis. Similarly, the speed of new atomic force microscopes allows for an entire coverslip of combed gDNA to be analyzed in minutes to hours, and are feasible to deploy for clinical diagnostics.

Such a diagnostic test could also be used to identify the molecular profile of BRCAness empirically rather than by relying solely on data mining from clinical resources such as the TCGA. Patient samples could be evaluated for ssDNA gaps by atomic force microscopy and subsequently sequenced to identify candidate BRCAness mutations. This dataset could then be combined with the mutation and expression data from large scale studies such as the TCGA and tested in laboratory cell culture experiments to build a robust BRCAness profile.

Technologies for Mechanistic Understanding

We also propose advanced technologies will be important to study BRCAness and DNA metabolism more generally. As discussed above, combing of DNA preserves many structures that are destroyed by current methods, and analysis by atomic force microscopy is of vastly higher resolution than what can be achieved by light microscopy. Light microscopy is resolution limited by diffraction to spheres of approximately 300nm; in contrast, the diameter of gDNA, depending on the support surface and conditions, is on the order of 2-10nm. Therefore, it is inevitable that substantial information about DNA structures and the replication fork are missing in light microscopy studies, and could be a vast oversimplification. Are single fluorescent tracks really representative of a single replication fork? Why, then, do the replication tracks appear as “beads on a string” - or are they really composed of multiple forks? Why does the first fluorescent label change length after therapy even when it is established before drug is added? Are the ssDNA regions we report really gaps in the DNA, or another structure? These are

critical questions that can only be answered by more sophisticated approaches. Moreover, atomic force microscopy can be combined with fluorescence microscopy in one instrument, and can even be used in aqueous conditions e.g. to observe enzymes, like S1, interacting with the DNA in picometer resolution movies with high framerates. Atomic force microscopy can also be used to detect the processing of DNA lesions over time, or to monitor ssDNA at timepoints distant from drug treatment, which cannot maintain the analog label.

Similarly, combing could lead to a substantial advance for electron microscopy analysis of DNA. gDNA is easily combed onto nanometer-thick silicon windows, which are molecularly similar to glass and are readily silanizable. With combing, intact gDNA can be deposited for analysis as discussed above; current electron microscopy methods require pipetting and digestion for deposition of DNA, which inevitably destroys vulnerable DNA structures. In addition, electron microscopy requires either labeling the DNA with heavy metals that bind to the backbone for transmission electron microscopy, or creation of a replica with rotary shadowing for scanning electron microscopy. Alternatively, could gDNA instead be combed onto a porous silicon window that has been silanized? In this case, the gDNA would be suspended over the pores - like a tightrope - in a vacuum, which is reported to lead to stunning resolution of unlabeled DNA[13]. With no heavy metal requirement, would we then be able to detect individual platinum lesions, which scatter electrons far more than the carbon-based DNA, and be able to discern the DNA structures created around them? Indeed, individual platinum atoms are readily detectable on carbon nanotubes, demonstrating the feasibility of the

goal[14]. Such an approach would be able to determine if platinum atoms were present in ssDNA regions, or at the ends of gDNA, which would indicate a double strand break, and would provide meaningful *physical* evidence to investigate the competing frameworks.

Limitations of Current Double Strand Break and ssDNA Techniques

In light of a new competing framework, we propose it will be important for future publications to discuss the limitations of the technical approaches used to measure DNA lesions and to explicitly address the inherent uncertainty in the techniques.

Pulsed Field Gel/Capillary Electrophoresis: We propose pulsed field experiments are currently the best techniques for the physical analysis of the length of gDNA polymers in order to directly detect double strand breaks. However, the assays are not without flaw; the techniques are sensitive but likely can only detect upwards of ten double strand breaks per cell. In addition, the gel is relatively qualitative and variable; the capillary version of the technique is quantitative and more consistent, but loading the gDNA onto the instrument likely induces double strand breaks that would be protected in the gel version of the technique. In addition, larger sizes of gDNA over approximately 1MB cannot reliably be distinguished in the capillary. An important limitation of both techniques is that they almost certainly also cause ssDNA regions to break during analysis; they cannot conclusively differentiate between a double strand break and a break caused in ssDNA due to handling or from being pulled through the matrix.

Comet Assays: Similar to pulsed field experiments, comet assays specifically measure the mobility of gDNA in a matrix and electric field. Although comet assays of varying conditions are described as being specific for double or single stranded breaks, we propose this language should be avoided. Indeed, both ssDNA and double strand breaks will increase the mobility of the gDNA through the matrix regardless of pH; this should be acknowledged in the discussions of results.

DNA Fiber Analysis and S1: We propose DNA fiber spreads should be replaced with DNA combing in order to obtain quantitative results, and these combed fibers should be analyzed by software to improve the rigor of the analysis for the modern age. Several limitations exist as described previously, most notably S1 activity against multiple DNA lesions that include loops; it will be important to directly observe ssDNA by electron microscopy or atomic force microscopy in order to accurately describe the lesion. For lesions many kilobases behind the fork, the emerging technique of combing with atomic force microscopy will likely prove superior to electron microscopy, which destroys the gDNA regions behind replication forks. Moreover, these physical techniques with their superior resolution will be an important complement to fluorescence microscopy. Indeed, fluorescence microscopy is limited to resolutions of approximately 300nm, whereas the diameter of DNA is approximately 2nm; it is nearly certain that light microscopy analysis of fibers is a drastic oversimplification.

yH2AX and Other Foci: We propose it will be important for the field to acknowledge that yH2AX and other proteins are not highly specific for a given DNA lesion, as proteins have a wide range of roles[15]. Foci analysis should be supported with a technique that physically analyzes the DNA polymer to detect the lesion, and we propose foci should not be used as a method for detecting low single digit numbers of double strand breaks or ssDNA[15].

The Evolutionary Role of ssDNA

As an appropriate conclusion, we note that our ssDNA theory made another surprising prediction: that *e. coli* and other bacteria would have an apoptotic pathway. Although we were unaware at the time, the presence of an apoptotic pathway in bacteria was highly disputed, and only became generally accepted sometime after 2015[16,17]. Accordingly, because genotoxins create double strand breaks in bacteria as well as in cancer cells, our theory lends support to this former controversy and has several interesting implications in the context of cancer.

The first problem was to determine why a single celled organism such as *e. coli* would have an apoptotic pathway to begin with. It appears this has been reconciled by the concept of altruism, which we largely agree with; an example given is the *e. coli* eject their DNA into a biofilm to protect the population when the individual has suffered too much DNA damage to continue. Other suggested advantages include saving resources - or passing resources to related group members. But a different possibility that would be less altruistic is shared between *e. coli* and cancers: gene transfer. Although

replicating seems to be the desired outcome, in the event of catastrophic DNA damage, it would be favorable for cells to be able to measure damage to know when replication was largely impossible and no longer worth pursuing – and to send the DNA to the lifeboats as a last ditch, and more effective, effort. This would likely require fragmenting the DNA so it can be exported out of the cell and transferred to healthy cells nearby – and this DNA fragmentation is conserved in apoptosis. Importantly, cancers almost certainly use this strategy for nefarious means – shedding of gDNA and other antigens into the microenvironment is a strategy to reprogram nearby healthy cells, or to tolerize the immune system for immune-evasion; the cancer is not bound by kin selection.

Single stranded DNA could be an easy lesion to create as such a measurement: determine when it is favorable for a cell to fragment the DNA and push it to the environment. This “measurement” aspect of ssDNA could explain why it seems omnipresent with DNA damage, and it would make sense that the ssDNA lesion would control programmed cell death rather than a more difficult lesion like a double strand break, especially considering DNA is an incredibly stable polymer. It should also require a substantial number of lesions to resort to apoptosis, for which ssDNA is well suited – it does not seem favorable for programmed cell death to be on a hair trigger, and this is consistent with experiment in human cancers.

More generally, the presence of such an apoptotic strategy places the BRCAness phenotype into a new perspective: the vulnerabilities of rapid replication may not be as one sided as we would like to believe.

APPENDIX

APPENDIX I: ***Atomic Force Microscopy on combed gDNA to measure ssDNA and lesions.*** I have developed a technique to measure combed gDNA via atomic force microscopy on a variety of silanized surfaces. The method will directly detect DNA forks and lesions, including ssDNA gaps, on combed gDNA at sub-nanometer resolution, and is able to detect the individual turns of the DNA double helix. Importantly, the combing approach applies less than 10pN of force and maximizes the gDNA structures that are preserved for analysis. In addition, atomic force microscopy can be combined with fluorescence imaging for analysis of labeled regions. To generate thin and stable silane coatings compatible with AFM, surfaces should be activated with an argon plasma for approximately ten minutes, and silanization should be applied by chemical vapor deposition for approximately ten minutes with the aid of a dry nitrogen bag to prevent polymerization. Importantly, the technique is compatible with nm thick TEM windows using air plasma, and the windows can even be successfully combed by using the silicon pad to mount the window to a coverslip for dipping; this surprising trick opens up the possibility of transmission electron microscopy analysis of combed gDNA.

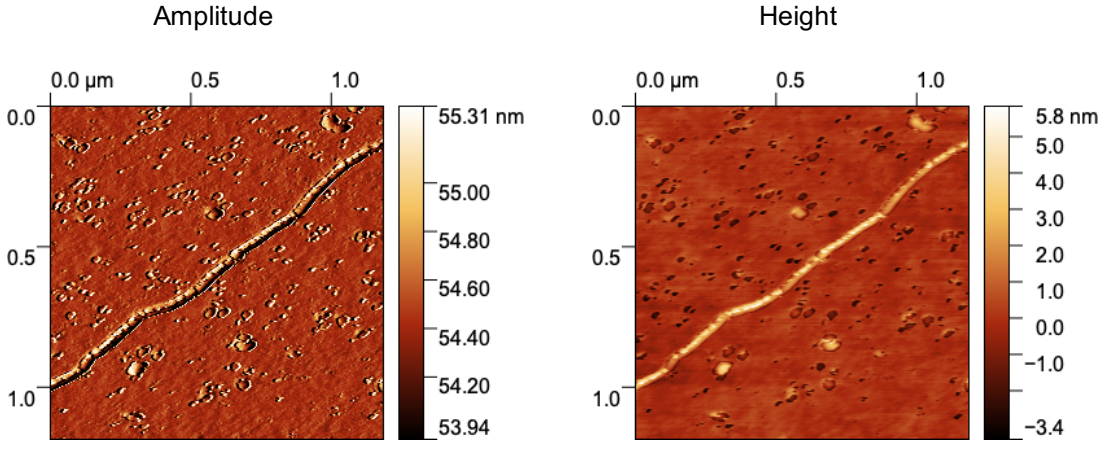

Appendix I: Analysis of combed gDNA by atomic force microscopy. Left, amplitude image of a combed gDNA fiber from BRCAness cells. The individual turns of the DNA helix are visible. Right, height image of same combed gDNA fiber. A literature search has been unable to find publications of AFM of combed gDNA on silanized surfaces, although early studies using lambda DNA are reported.

APPENDIX II: *Bioinformatics Tools for TCGA patient analysis and modeling.* I have developed a set of Python tools to automate the TCGA survival analysis described in *Panzarino et al.* The tools rapidly identify clinically relevant candidate genes for therapy response *in silico.* The code groups patients of interest by high and low expression for all ~12,000 reported genes, followed by survival analysis with *lifelines* and p-value determination; importantly, the area under the survival curve is superior to graphing the IC50 value due to the data distribution. The full six-hundred ovarian cancer patient cohort can be analyzed in approximately ten minutes. This approach can be merged with other techniques, including mass spectrometry proteomics and shRNA screens, to model and elucidate detailed mechanisms of chemoresponse, including a possible *BRCAness* signature, in a modern, systems biology manner.

1. Panzarino, N. J. *et al.* Replication Gaps Underlie BRCA Deficiency and Therapy Response. *Cancer Research.* 2021.

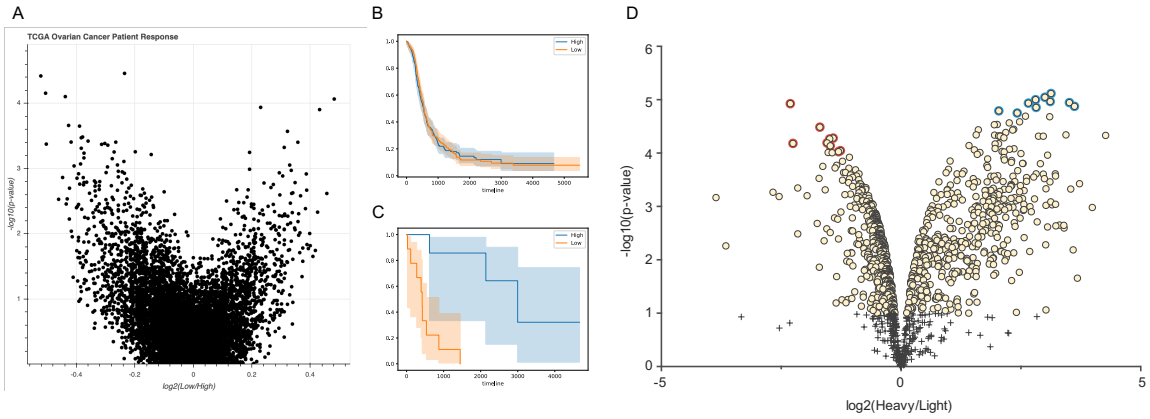

Appendix II*:* Bioinformatics tools to model TCGA patient response. A) The unbiased model of tumor genes that predict therapy response in BRCA2 deficient ovarian cancer patients. B) The gene PHC2 has no apparent predictive power in the full ovarian cancer group, but in the BRCA2 germline group, C), PHC2 mRNA displays one of the highest predictive powers of all genes included in the TCGA for this subset. PHC2 was identified using these tools without bias, *i.e.* without a hypothesis; we have successfully identified the predictive power of all 12,000 genes in the BRCA2 germline subset. Survival of each group is determined by integration (area under the survival curve). D) The TCGA survival predictions can be combined with mass spectrometry to construct protein models of therapy response that can be validated by shRNA; here the nuclear fraction of PEO1 (Heavy) vs C4-2 (Light) as published.

APPENDIX III: ***Replication fork protection confers genome stability and chemotherapeutic resistance.*** In a collaboration with A. Chaudhuri and A. Nussenzweig, we published that stabilized replication forks confer chemoresistance in BRCA2 deficient cells when CHD4 is depleted (A). We found forks were stabilized likely because MRE11 foci and chromatin localization had been eliminated (B, C, D), which implicated MRE11 as the nuclease that degrades forks into double strand breaks to confer hypersensitivity as predicted by the dogma. As controls, we confirmed CHD4 depletion did not alter the cell cycle or reduce total MRE11 levels (E, F). N. Panzarino created panels B, C, D, F, and assisted with A and E; D is unpublished.

1. Chaudhuri, A. R. *et al.* Replication fork stability confers chemoresistance in BRCA-deficient cells. *Nature* **535**, 382–7 (2016).

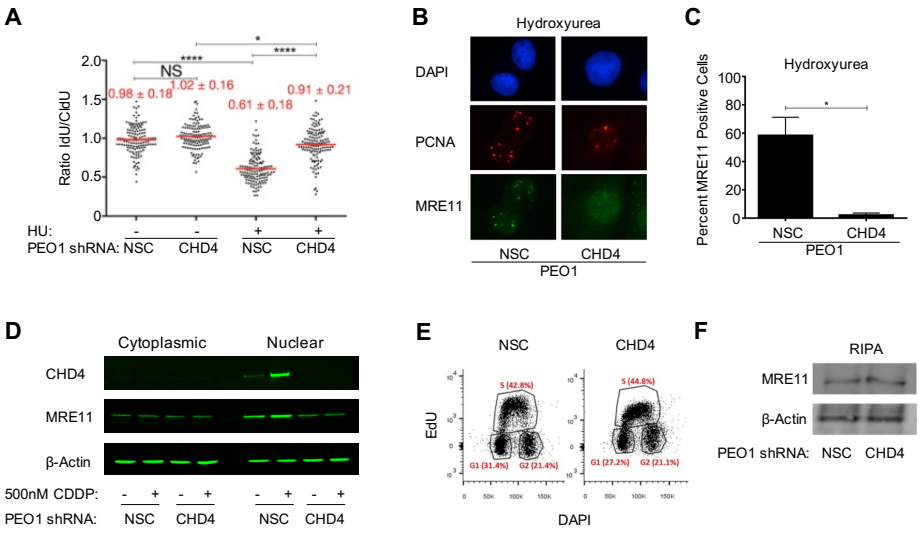

Appendix III: Replication fork protection confers chemotherapeutic resistance. A) Fiber ratio of IdU versus CldU in BRCA2-mutated PEO1 cells either mock (shNSC) infected or infected with shRNA against CHD4 (shCHD4). One hundred and twenty-five replication forks were analysed. B) Immunostaining for MRE11 and PCNA in PEO1 cells infected with shNSC and shCHD4 upon treatment with 4 mM HU; C), quantification for MRE11 recruitment upon HU treatment. At least 100 cells were analysed per condition; experiments were repeated three times. D) Near infrared western blot for MRE11 in PEO1 cells infected with shNSC and shCHD4 after 500nM CDDP for 18h. E) Cell cycle profiles in PEO1 cells infected with shNSC and shCHD4 as measured by the incorporation of EdU versus DAPI. F) Western blot analysis for CHD4 and MRE11 levels in PEO1 cells infected with shNSC and shCHD4.

BIBLIOGRAPHY

Chapter I: Introduction

1. Hall, J. et al. Linkage of early-onset familial breast cancer to chromosome 17q21. Science 250, 1684–1689 (1990).

2. Miki, Y. et al. A strong candidate for the breast and ovarian cancer susceptibility gene BRCA1. Science 266, 66–71 (1994).

3. Wooster, R. et al. Localization of a breast cancer susceptibility gene, BRCA2, to chromosome 13q12-13. Science 265, 2088–2090 (1994).

4. Wooster, R. et al. Identification of the breast cancer susceptibility gene BRCA2. Nature 378, 789–792 (1995).

5. Bhattacharyya, A., Ear, U. S., Koller, B. H., Weichselbaum, R. R. & Bishop, D. K. The Breast Cancer Susceptibility Gene BRCA1 Is Required for Subnuclear Assembly of Rad51 and Survival following Treatment with the DNA Cross-linking Agent Cisplatin*. J Biol Chem 275, 23899–23903 (2000).

6. Scully, R. et al. Genetic Analysis of BRCA1 Function in a Defined Tumor Cell Line. Mol Cell 4, 1093–1099 (1999).

7. Sakai, W. et al. Secondary mutations as a mechanism of cisplatin resistance in BRCA2-mutated cancers. Nature 451, 1116–1120 (2008).

8. Fedier, A. et al. The effect of loss of Brca1 on the sensitivity to anticancer agents in p53-deficient cells. Int J Oncol 22, 1169–73 (2003).

9. Scully, R. et al. Association of BRCA1 with Rad51 in Mitotic and Meiotic Cells. Cell 88, 265–275 (1997).

10. Scully, R. et al. Dynamic Changes of BRCA1 Subnuclear Location and Phosphorylation State Are Initiated by DNA Damage. Cell 90, 425–435 (1997).

11. Liu, Q. et al. Loss of TGFβ signaling increases alternative end-joining DNA repair that sensitizes to genotoxic therapies across cancer types. Sci Transl Med 13, eabc4465 (2021).

12. Liang, F., Han, M., Romanienko, P. J. & Jasin, M. Homology-directed repair is a major double-strand break repair pathway in mammalian cells. Proc National Acad Sci 95, 5172–5177 (1998).

13. Moynahan, M. E., Chiu, J. W., Koller, B. H. & Jasin, M. Brca1 Controls Homology-Directed DNA Repair. Mol Cell 4, 511–518 (1999).

14. Nowosielska, A., Calmann, M. A., Zdraveski, Z., Essigmann, J. M. & Marinus, M. G. Spontaneous and cisplatin-induced recombination in Escherichia coli. Dna Repair 3, 719–728 (2004).

15. Nowosielska, A. & Marinus, M. G. Cisplatin induces DNA double-strand break formation in Escherichia coli dam mutants. Dna Repair 4, 773–781 (2005).

16. Ryan, A. J., Squires, S., Strutt, H. L. & Johnson, R. T. Camptothecin cytotoxicity in mammalian cells is associated with the induction of persistent double strand breaks in replicating DNA. Nucleic Acids Res 19, 3295–3300 (1991).

17. Ormerod, M. G., O'Neill, C. F., Robertson, D. & Harrap, K. R. Cisplatin Induces Apoptosis in a Human Ovarian Carcinoma Cell Line without Concomitant Internucleosomal Degradation of DNA. Exp Cell Res 211, 231–237 (1994).

18. Rosenberg, B. Charles F. Kettring prize. Fundamental studies with cisplatin. Cancer 55, 2303–2316 (1985).

19. Hsiang, Y. H., Hertzberg, R., Hecht, S. & Liu, L. F. Camptothecin induces protein-linked DNA breaks via mammalian DNA topoisomerase I. J Biol Chem 260, 14873–14878 (1985).

20. Donahue, S. L. & Campbell, C. A DNA Double Strand Break Repair Defect in Fanconi Anemia Fibroblasts*. J Biol Chem 277, 46243–46247 (2002).

21. Farmer, H. et al. Targeting the DNA repair defect in BRCA mutant cells as a therapeutic strategy. Nature 434, 917–921 (2005).

22. Bryant, H. E. et al. Specific killing of BRCA2-deficient tumours with inhibitors of poly(ADP-ribose) polymerase. Nature 434, 913–917 (2005).

23. Turner, N., Tutt, A. & Ashworth, A. Hallmarks of "BRCAness" in sporadic cancers. Nat Rev Cancer 4, 814–819 (2004).

24. Schlacher, K. et al. Double-strand break repair-independent role for BRCA2 in blocking stalled replication fork degradation by MRE11. Cell 145, 529–42 (2011).

25. Schlacher, K., Wu, H. & Jasin, M. A Distinct Replication Fork Protection Pathway Connects Fanconi Anemia Tumor Suppressors to RAD51-BRCA1/2. Cancer Cell 22, 106–116 (2012).

26. Chaudhuri, A. R. et al. Replication fork stability confers chemoresistance in BRCA-deficient cells. Nature 535, 382–7 (2016).

27. Guillemette, S. et al. Resistance to therapy in BRCA2 mutant cells due to loss of the nucleosome remodeling factor CHD4. Gene Dev 29, 489–494 (2015).

28. Rondinelli, B. et al. EZH2 promotes degradation of stalled replication forks by recruiting MUS81 through histone H3 trimethylation. Nat Cell Biol 19, 1371–1378 (2017).

29. Meghani, K. et al. Multifaceted Impact of MicroRNA 493-5p on Genome-Stabilizing Pathways Induces Platinum and PARP Inhibitor Resistance in BRCA2-Mutated Carcinomas. Cell Reports 23, 100–111 (2018).

30. Taglialatela, A. et al. Restoration of Replication Fork Stability in BRCA1- and BRCA2-Deficient Cells by Inactivation of SNF2-Family Fork Remodelers. Mol Cell 68, 414-430.e8 (2017).

31. Kolinjivadi, A. M. et al. Smarcal1-Mediated Fork Reversal Triggers Mre11-Dependent Degradation of Nascent DNA in the Absence of Brca2 and Stable Rad51 Nucleofilaments. Mol Cell 67, 867-881.e7 (2017).

32. Cantor, S. B. & Calvo, J. A. Fork Protection and Therapy Resistance in Hereditary Breast Cancer. Cold Spring Harb Sym 82, 339–348 (2017).

33. Bhat, K. P. et al. RADX Modulates RAD51 Activity to Control Replication Fork Protection. Cell Reports 24, 538–545 (2018).

34. Wang, A. T. et al. A Dominant Mutation in Human RAD51 Reveals Its Function in DNA Interstrand Crosslink Repair Independent of Homologous Recombination. Mol Cell 59, 478–490 (2015).

35. Lossaint, G. et al. FANCD2 Binds MCM Proteins and Controls Replisome Function upon Activation of S Phase Checkpoint Signaling. Mol Cell 51, 678–690 (2013).

36. Panzarino, N. J. et al. Replication Gaps Underlie BRCA Deficiency and Therapy Response. Cancer Res 81, 1388–1397 (2021).

37. Dyson, F. W., Eddington, A. S. & Davidson, C. IX. A determination of the deflection of light by the sun’s gravitational field, from observations made at the total eclipse of May 29, 1919. Philosophical Transactions Royal Soc Lond Ser Contain Pap Math Or Phys Character 220, 291–333 (1920).

38. Sakahira, H., Enari, M. & Nagata, S. Cleavage of CAD inhibitor in CAD activation and DNA degradation during apoptosis. Nature 391, 96–99 (1998).

39. Kawane, K., Motani, K. & Nagata, S. DNA Degradation and Its Defects. Csh Perspect Biol 6, a016394 (2014).

40. Dwyer, D. J., Camacho, D. M., Kohanski, M. A., Callura, J. M. & Collins, J. J. Antibiotic-Induced Bacterial Cell Death Exhibits Physiological and Biochemical Hallmarks of Apoptosis. Mol Cell 46, 561–572 (2012).

41. Bos, J., Yakhnina, A. A. & Gitai, Z. BapE DNA endonuclease induces an apoptotic-like response to DNA damage in Caulobacter. Proc National Acad Sci 109, 18096–18101 (2012).

42. Bayles, K. W. Bacterial programmed cell death: making sense of a paradox. Nat Rev Microbiol 12, 63–69 (2014).

43. Yeung, T. et al. Avoidance of apoptotic death via a hyperploid salvage survival pathway after platinum treatment in high grade serous carcinoma cell line models. Oncotarget 10, 6691–6712 (2019).

44. Shimizu, T. & Pommier, Y. Camptothecin-induced apoptosis in p53-null human leukemia HL60 cells and their isolated nuclei: effects of the protease inhibitors Z-VAD-fmk and dichloroisocoumarin suggest an involvement of both caspases and serine proteases. Leukemia 11, 1238–1244 (1997).

45. Sané, A. T. & Bertrand, R. Distinct steps in DNA fragmentation pathway during camptothecin-induced apoptosis involved caspase-, benzyloxycarbonyl- and N-tosyl-L-phenylalanylchloromethyl ketone-sensitive activities. Cancer Res 58, 3066–72 (1998).

46. Ceccaldi, R. et al. Homologous-recombination-deficient tumours are dependent on Polθ-mediated repair. Nature 518, 258–262 (2015).

47. Cong, K. et al. PARPi synthetic lethality derives from replication-associated single-stranded DNA gaps. Biorxiv 781989 (2019) doi:10.1101/781989.

48. González-Martín, A. et al. Niraparib in Patients with Newly Diagnosed Advanced Ovarian Cancer. New Engl J Med 381, 2391–2402 (2019).

49. Zimmer, A. S., Gillard, M., Lipkowitz, S. & Lee, J.-M. Update on PARP Inhibitors in Breast Cancer. Curr Treat Option On 19, 21 (2018).

50. Coleman, R. L. et al. Veliparib with First-Line Chemotherapy and as Maintenance Therapy in Ovarian Cancer. New Engl J Med 381, 2403–2415 (2019).

51. Bono, J. de et al. Olaparib for Metastatic Castration-Resistant Prostate Cancer. New Engl J Med 382, 2091–2102 (2020).

52. Nayak, S. et al. Inhibition of the translesion synthesis polymerase REV1 exploits replication gaps as a cancer vulnerability. Sci Adv 6, eaaz7808 (2020).

53. Quinet, A., Tirman, S., Cybulla, E., Meroni, A. & Vindigni, A. To skip or not to skip: choosing repriming to tolerate DNA damage. Mol Cell 81, 649–658 (2021).

54. Kwak, K. J., Kudo, H. & Fujihira, M. Imaging stretched single DNA molecules by pulsed-force-mode atomic force microscopy. Ultramicroscopy 97, 249–255 (2003).

55. Michalet, X. et al. Dynamic Molecular Combing: Stretching the Whole Human Genome for High-Resolution Studies. Science 277, 1518–1523 (1997).

56. Bensimon, A. et al. Alignment and sensitive detection of DNA by a moving interface. Science 265, 2096–2098 (1994).

57. Sawyer, S. L. et al. Biallelic Mutations in BRCA1 Cause a New Fanconi Anemia Subtype. Cancer Discov 5, 135–142 (2015).

58. Howlett, N. G. et al. Biallelic Inactivation of BRCA2 in Fanconi Anemia. Science 297, 606–609 (2002).

59. Somyajit, K. et al. Homology-directed repair protects the replicating genome from metabolic assaults. Dev Cell 56, 461-477.e7 (2021).

60. Reid-Bayliss, K. S., Arron, S. T., Loeb, L. A., Bezrookove, V. & Cleaver, J. E. Why Cockayne syndrome patients do not get cancer despite their DNA repair deficiency. Proc National Acad Sci 113, 10151–10156 (2016).

61. Karaayvaz-Yildirim, M. et al. Aneuploidy and a deregulated DNA damage response suggest haploinsufficiency in breast tissues of BRCA2 mutation carriers. Sci Adv 6, eaay2611 (2020).

Chapter II: Results

1. M. C. King et al., Genetic analysis of human breast cancer: literature review and description of family data in workshop. Genet Epidemiol Suppl 1, 3-13 (1986).

2. E. W. Munnell, The changing prognosis and treatment in cancer of the ovary. A report of 235 patients with primary ovarian carcinoma 1952-1961. Am J Obstet Gynecol 100, 790-805 (1968).

3. X. Li, W. D. Heyer, Homologous recombination in DNA repair and DNA damage tolerance. Cell Res 18, 99-113 (2008).

4. W. Feng, M. Jasin, Homologous Recombination and Replication Fork Protection: BRCA2 and More! Cold Spring Harb Symp Quant Biol 82, 329-338 (2017).

5. M. Lomonosov, S. Anand, M. Sangrithi, R. Davies, A. R. Venkitaraman, Stabilization of stalled DNA replication forks by the BRCA2 breast cancer susceptibility protein. Genes Dev 17, 3017- 3022 (2003).

6. K. Schlacher et al., Double-strand break repair-independent role for BRCA2 in blocking stalled replication fork degradation by MRE11. Cell 145, 529-542 (2011).

7. K. Schlacher, H. Wu, M. Jasin, A distinct replication fork protection pathway connects Fanconi anemia tumor suppressors to RAD51-BRCA1/2. Cancer cell 22, 106-116 (2012).

8. J. Huang et al., The DNA translocase FANCM/MHF promotes replication traverse of DNA interstrand crosslinks. Molecular cell 52, 434-446 (2013).

9. K. Mutreja et al., ATR-Mediated Global Fork Slowing and Reversal Assist Fork Traverse and Prevent Chromosomal Breakage at DNA Interstrand Cross-Links. Cell Rep 24, 2629-2642 e2625 (2018).

10. S. B. Cantor, J. A. Calvo, Fork Protection and Therapy Resistance in Hereditary Breast Cancer. Cold Spring Harb Symp Quant Biol, (2018).

11. S. F. Bunting et al., BRCA1 Functions Independently of Homologous Recombination in DNA Interstrand Crosslink Repair. Molecular cell 46, 125-135 (2012).

12. A. T. Wang et al., A Dominant Mutation in Human RAD51 Reveals Its Function in DNA Interstrand Crosslink Repair Independent of Homologous Recombination. Mol Cell 59, 478-490 (2015).

13. M. Barazas et al., Radiosensitivity Is an Acquired Vulnerability of PARPi-Resistant BRCA1- Deficient Tumors. Cancer Res 79, 452-460 (2019).

14. P. M. Bruno et al., A subset of platinum-containing chemotherapeutic agents kills cells by inducing ribosome biogenesis stress. Nat Med 23, 461-471 (2017).

15. A. M. Heijink et al., Modeling of Cisplatin-Induced Signaling Dynamics in Triple-Negative Breast Cancer Cells Reveals Mediators of Sensitivity. Cell Rep 28, 2345-2357 e2345 (2019).

16. J. Schindelin et al., Fiji: an open-source platform for biological-image analysis. Nat Methods 9, 676-682 (2012).

17. A. Koc, L. J. Wheeler, C. K. Mathews, G. F. Merrill, Hydroxyurea arrests DNA replication by a mechanism that preserves basal dNTP pools. J Biol Chem 279, 223-230 (2004).

18. A. R. Chaudhuri et al., Replication fork stability confers chemoresistance in BRCA-deficient cells. Nature 535, 382-387 (2016).

19. W. Sakai et al., Functional restoration of BRCA2 protein by secondary BRCA2 mutations in BRCA2-mutated ovarian carcinoma. Cancer Res 69, 6381-6386 (2009).

20. A. Quinet, D. Carvajal-Maldonado, D. Lemacon, A. Vindigni, DNA Fiber Analysis: Mind the Gap! Methods Enzymol 591, 55-82 (2017).

21. S. Guillemette et al., Resistance to therapy in BRCA2 mutant cells due to loss of the nucleosome remodeling factor CHD4. Genes Dev 29, 489-494 (2015).

22. A. O'Shaughnessy, B. Hendrich, CHD4 in the DNA-damage response and cell cycle progression: not so NuRDy now. Biochemical Society transactions 41, 777-782 (2013).

23. B. Rondinelli et al., EZH2 promotes degradation of stalled replication forks by recruiting MUS81 through histone H3 trimethylation. Nat Cell Biol 19, 1371-1378 (2017).

24. K. Meghani et al., Multifaceted Impact of MicroRNA 493-5p on Genome-Stabilizing Pathways Induces Platinum and PARP Inhibitor Resistance in BRCA2-Mutated Carcinomas. Cell Rep 23, 100-111 (2018).

25. K. E. Mengwasser et al., Genetic Screens Reveal FEN1 and APEX2 as BRCA2 Synthetic Lethal Targets. Mol Cell 73, 885-899 e886 (2019).

26. Y. Chudnovsky et al., ZFHX4 interacts with the NuRD core member CHD4 and regulates the glioblastoma tumor-initiating cell state. Cell Rep 6, 313-324 (2014).

27. A. Taglialatela et al., Restoration of Replication Fork Stability in BRCA1- and BRCA2-Deficient Cells by Inactivation of SNF2-Family Fork Remodelers. Mol Cell 68, 414-430 e418 (2017).

28. A. M. Kolinjivadi et al., Smarcal1-Mediated Fork Reversal Triggers Mre11-Dependent Degradation of Nascent DNA in the Absence of Brca2 and Stable Rad51 Nucleofilaments. Mol Cell 67, 867-881 e867 (2017).

29. K. P. Bhat et al., RADX Modulates RAD51 Activity to Control Replication Fork Protection. Cell Rep 24, 538-545 (2018).

30. R. Zellweger et al., Rad51-mediated replication fork reversal is a global response to genotoxic treatments in human cells. J Cell Biol 208, 563-579 (2015).

31. C. J. Van Noorden, The history of Z-VAD-FMK, a tool for understanding the significance of caspase inhibition. Acta Histochem 103, 241-251 (2001).

32. J. Henry-Mowatt et al., XRCC3 and Rad51 modulate replication fork progression on damaged vertebrate chromosomes. Mol Cell 11, 1109-1117 (2003).

33. K. Sugimura, S. Takebayashi, H. Taguchi, S. Takeda, K. Okumura, PARP-1 ensures regulation of replication fork progression by homologous recombination on damaged DNA. J Cell Biol 183, 1203-1212 (2008).

34. X. Su, J. A. Bernal, A. R. Venkitaraman, Cell-cycle coordination between DNA replication and recombination revealed by a vertebrate N-end rule degron-Rad51. Nat Struct Mol Biol 15, 1049-1058 (2008).

35. Y. Hashimoto, A. Ray Chaudhuri, M. Lopes, V. Costanzo, Rad51 protects nascent DNA from Mre11-dependent degradation and promotes continuous DNA synthesis. Nat Struct Mol Biol 17, 1305-1311 (2010).

36. S. Luke-Glaser, B. Luke, S. Grossi, A. Constantinou, FANCM regulates DNA chain elongation and is stabilized by S-phase checkpoint signalling. EMBO J 29, 795-805 (2010).

37. M. B. Vallerga, S. F. Mansilla, M. B. Federico, A. P. Bertolin, V. Gottifredi, Rad51 recombinase prevents Mre11 nuclease-dependent degradation and excessive PrimPol-mediated elongation of nascent DNA after UV irradiation. Proc Natl Acad Sci U S A 112, E6624-6633 (2015).

38. A. M. Kolinjivadi et al., Moonlighting at replication forks - a new life for homologous recombination proteins BRCA1, BRCA2 and RAD51. FEBS Lett 591, 1083-1100 (2017).

39. R. P. Wong, N. Garcia-Rodriguez, N. Zilio, M. Hanulova, H. D. Ulrich, Processing of DNA Polymerase-Blocking Lesions during Genome Replication Is Spatially and Temporally Segregated from Replication Forks. Mol Cell, (2019).

40. I. Elvers, F. Johansson, P. Groth, K. Erixon, T. Helleday, UV stalled replication forks restart by re-priming in human fibroblasts. Nucleic Acids Res 39, 7049-7057 (2011).

41. S. Mouron et al., Repriming of DNA synthesis at stalled replication forks by human PrimPol. Nat Struct Mol Biol 20, 1383-1389 (2013).

42. J. Bianchi et al., PrimPol bypasses UV photoproducts during eukaryotic chromosomal DNA replication. Mol Cell 52, 566-573 (2013).

43. X. Xu et al., BRCA1 represses DNA replication initiation through antagonizing estrogen signaling and maintains genome stability in parallel with WEE1-MCM2 signaling during pregnancy. Hum Mol Genet, (2018).

44. S. Mijic et al., Replication fork reversal triggers fork degradation in BRCA2-defective cells. Nature communications 8, 859 (2017).

45. M. Zimmermann et al., CRISPR screens identify genomic ribonucleotides as a source of PARP-trapping lesions. Nature 559, 285-289 (2018).

46. S. Faivre, D. Chan, R. Salinas, B. Woynarowska, J. M. Woynarowski, DNA strand breaks and apoptosis induced by oxaliplatin in cancer cells. Biochem Pharmacol 66, 225-237 (2003).

47. A. T. Sane, R. Bertrand, Distinct steps in DNA fragmentation pathway during camptothecin-induced apoptosis involved caspase-, benzyloxycarbonyl- and N-tosyl-L-phenylalanylchloromethyl ketone-sensitive activities. Cancer Res 58, 3066-3072 (1998).

48. A. Nowosielska, M. G. Marinus, Cisplatin induces DNA double-strand break formation in Escherichia coli dam mutants. DNA repair 4, 773-781 (2005).

49. K. Kawane, K. Motani, S. Nagata, DNA degradation and its defects. Cold Spring Harb Perspect Biol 6, (2014).

50. H. Sakahira, M. Enari, S. Nagata, Cleavage of CAD inhibitor in CAD activation and DNA degradation during apoptosis. Nature 391, 96-99 (1998).

51. L. C. Huang, K. C. Clarkin, G. M. Wahl, Sensitivity and selectivity of the DNA damage sensor responsible for activating p53-dependent G1 arrest. Proc Natl Acad Sci U S A 93, 4827-4832 (1996).

52. D. M. Tidd et al., Oligodeoxynucleotide 5mers containing a 5'-CpG induce apoptosis through a mitochondrial mechanism in T lymphocytic leukaemia cells. Nucleic Acids Res 28, 2242-2250 (2000).

53. S. Nayak et al., Inhibition of the translesion synthesis polymerase REV1 exploits replication gaps as a cancer vulnerability. Sci Adv 6, eaaz7808 (2020).

54. P. Tonzi, T. T. Huang, Role of Y-family translesion DNA polymerases in replication stress: Implications for new cancer therapeutic targets. DNA Repair (Amst) 78, 20-26 (2019).

55. K. Cong et al., PARPi synthetic lethality derives from replication-associated single-stranded DNA gaps. bioRxiv, 781989 (2019).

Supplemental Methods

1. K. Schlacher et al., Double-strand break repair-independent role for BRCA2 in blocking stalled replication fork degradation by MRE11. Cell 145, 529-542 (2011).

2. B. Rondinelli et al., EZH2 promotes degradation of stalled replication forks by recruiting MUS81 through histone H3 trimethylation. Nat Cell Biol 19, 1371-1378 (2017).

3. S. Guillemette et al., Resistance to therapy in BRCA2 mutant cells due to loss of the nucleosome remodeling factor CHD4. Genes Dev 29, 489-494 (2015).

4. A. Bensimon et al., Alignment and sensitive detection of DNA by a moving interface. Science 265, 2096-2098 (1994).

5. A. E. Carpenter et al., CellProfiler: image analysis software for identifying and quantifying cell phenotypes. Genome Biol 7, R100 (2006).

6. M. Peng et al., Opposing Roles of FANCJ and HLTF Protect Forks and Restrain Replication during Stress. Cell Rep 24, 3251-3261 (2018).

7. J. Cox, M. Mann, MaxQuant enables high peptide identification rates, individualized p.p.b.-range mass accuracies and proteome-wide protein quantification. Nat Biotechnol 26, 1367-1372 (2008).

8. M. E. Ritchie et al., limma powers differential expression analyses for RNA-sequencing and microarray studies. Nucleic Acids Res 43, e47 (2015).

9. H. Li et al., The Sequence Alignment/Map format and SAMtools. Bioinformatics 25, 2078-2079 (2009).

10. A. McKenna et al., The Genome Analysis Toolkit: a MapReduce framework for analyzing next-generation DNA sequencing data. Genome Res 20, 1297-1303 (2010).

11. W. McLaren et al., The Ensembl Variant Effect Predictor. Genome Biol 17, 122 (2016).

12. J. Liu et al., An Integrated TCGA Pan-Cancer Clinical Data Resource to Drive High-Quality Survival Outcome Analytics. Cell 173, 400-416 e411 (2018).

13. E. Cerami et al., The cBio cancer genomics portal: an open platform for exploring multidimensional cancer genomics data. Cancer Discov 2, 401-404 (2012).

14. J. Gao et al., Integrative analysis of complex cancer genomics and clinical profiles using the cBioPortal. Sci Signal 6, pl1 (2013).

15. J. K. Cameron Davidson-Pilon, Noah Jacobson, sean-reed, Ben Kuhn, Paul Zivich, in Zenodo. http://doi.org/10.5281/zenodo.4136578. (2020).

16. C. M. Doskey, T. J. van 't Erve, B. A. Wagner, G. R. Buettner, Moles of a Substance per Cell Is a Highly Informative Dosing Metric in Cell Culture. PLoS One 10, e0132572 (2015).

Chapter III: Discussion

1. Floyd, S. R. et al. The bromodomain protein Brd4 insulates chromatin from DNA damage signalling. Nature 498, 246–250 (2013).

2. Karaayvaz-Yildirim, M. et al. Aneuploidy and a deregulated DNA damage response suggest haploinsufficiency in breast tissues of BRCA2 mutation carriers. Sci Adv 6, eaay2611 (2020).

3. Somyajit, K. et al. Homology-directed repair protects the replicating genome from metabolic assaults. Dev Cell 56, 461-477.e7 (2021).

4. Reid-Bayliss, K. S., Arron, S. T., Loeb, L. A., Bezrookove, V. & Cleaver, J. E. Why Cockayne syndrome patients do not get cancer despite their DNA repair deficiency. Proc National Acad Sci 113, 10151–10156 (2016).

5. Kwak, K. J., Kudo, H. & Fujihira, M. Imaging stretched single DNA molecules by pulsed-force-mode atomic force microscopy. Ultramicroscopy 97, 249–255 (2003).

6. Sage, J. M. & Knight, K. L. Human Rad51 promotes mitochondrial DNA synthesis under conditions of increased replication stress. Mitochondrion 13, 350–356 (2013).

7. Phillips, A. F. et al. Single-Molecule Analysis of mtDNA Replication Uncovers the Basis of the Common Deletion. Mol Cell 65, 527-538.e6 (2017).

8. Han, C. et al. Tumor cells suppress radiation-induced immunity by hijacking caspase 9 signaling. Nat Immunol 21, 546–554 (2020).

9. Chan, H. L. et al. Polycomb complexes associate with enhancers and promote oncogenic transcriptional programs in cancer through multiple mechanisms. Nat Commun 9, 3377 (2018).

10. Sparmann, A. et al. The chromodomain helicase Chd4 is required for Polycomb-mediated inhibition of astroglial differentiation. Embo J 32, 1598–1612 (2013).

11. Bensimon, A. et al. Alignment and sensitive detection of DNA by a moving interface. Science 265, 2096–2098 (1994).

12. Michalet, X. et al. Dynamic Molecular Combing: Stretching the Whole Human Genome for High-Resolution Studies. Science 277, 1518–1523 (1997).

13. Gentile, F. et al. Direct Imaging of DNA Fibers: The Visage of Double Helix. Nano Lett 12, 6453–6458 (2012).

14. Bhirde, A. A. et al. Imaging the distribution of individual platinum-based anticancer drug molecules attached to single-wall carbon nanotubes. Nanomedicine-uk 4, 763–772 (2009).

15. Feraudy, S. de, Revet, I., Bezrookove, V., Feeney, L. & Cleaver, J. E. A minority of foci or pan-nuclear apoptotic staining of γH2AX in the S phase after UV damage contain DNA double-strand breaks. Proc National Acad Sci 107, 6870–6875 (2010).

16. Bayles, K. W. Are the molecular strategies that control apoptosis conserved in bacteria? Trends Microbiol 11, 306–311 (2003).

17. Bayles, K. W. Bacterial programmed cell death: making sense of a paradox. Nat Rev Microbiol 12, 63–69 (2014).